

Peering into the most massive star in the Galaxy with near-infrared interferometry



Image credits: Montage (J. Groh), VLTI (ESO), Eta Car (N. Smith + NASA)

Jose Groh (Geneva Observatory, Switzerland)

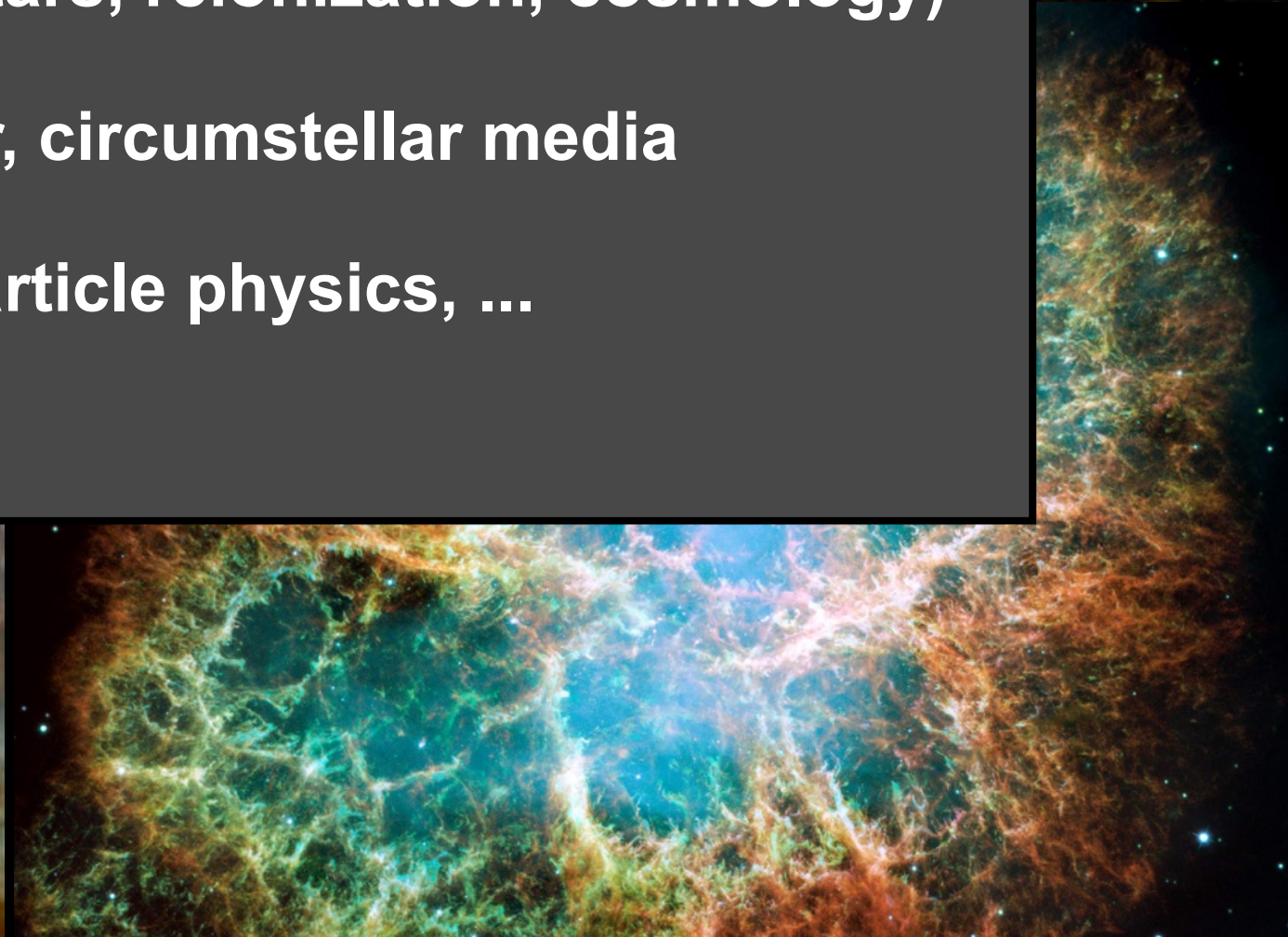
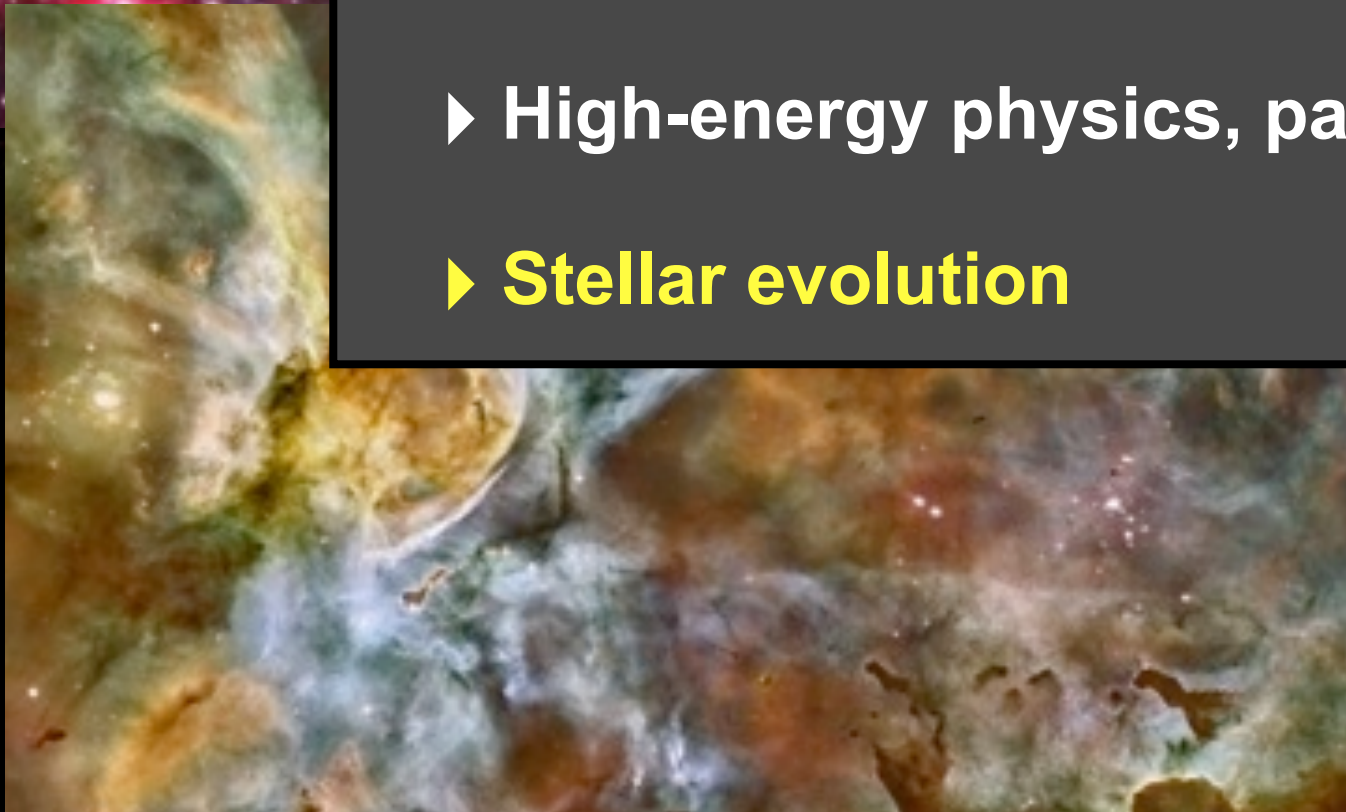
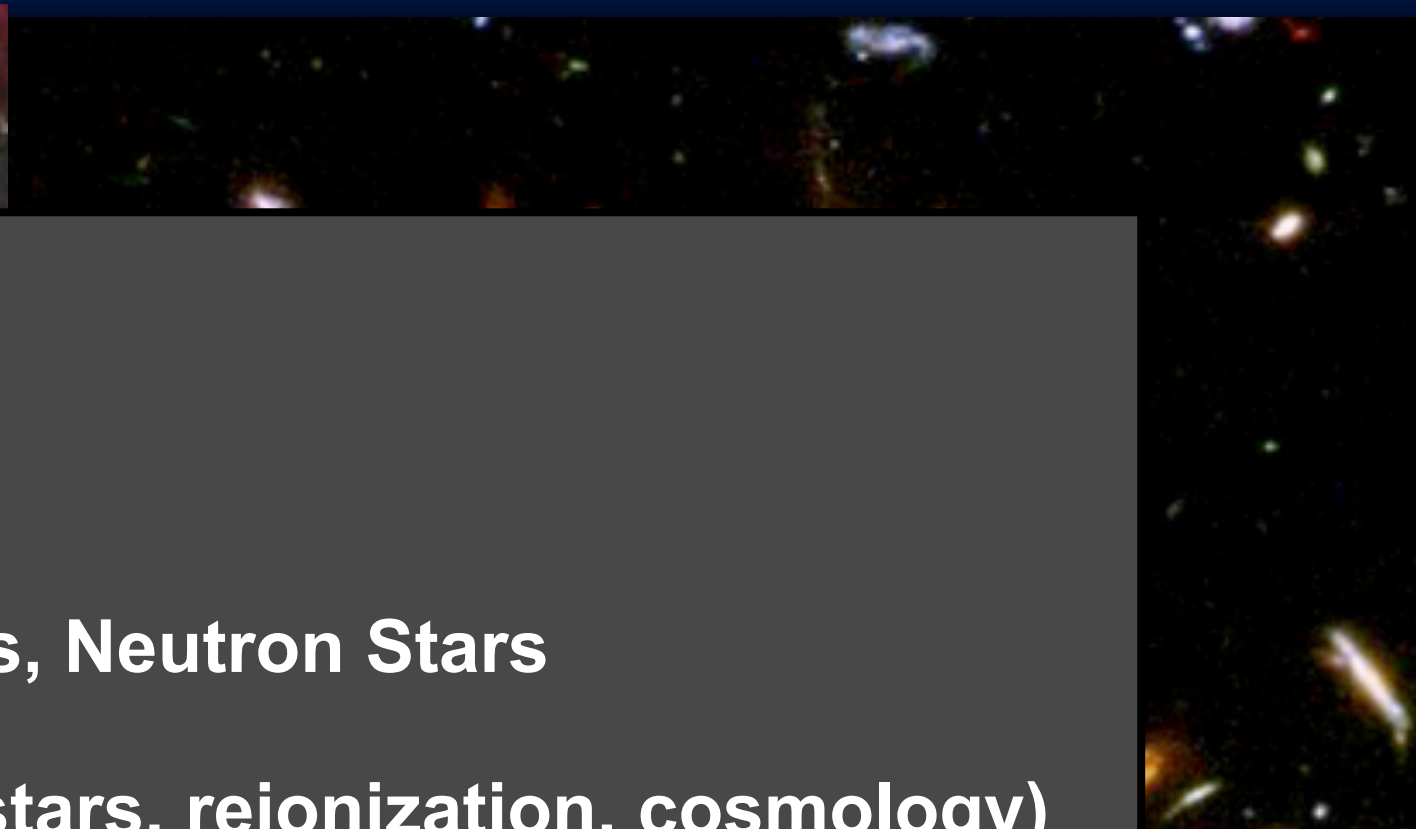
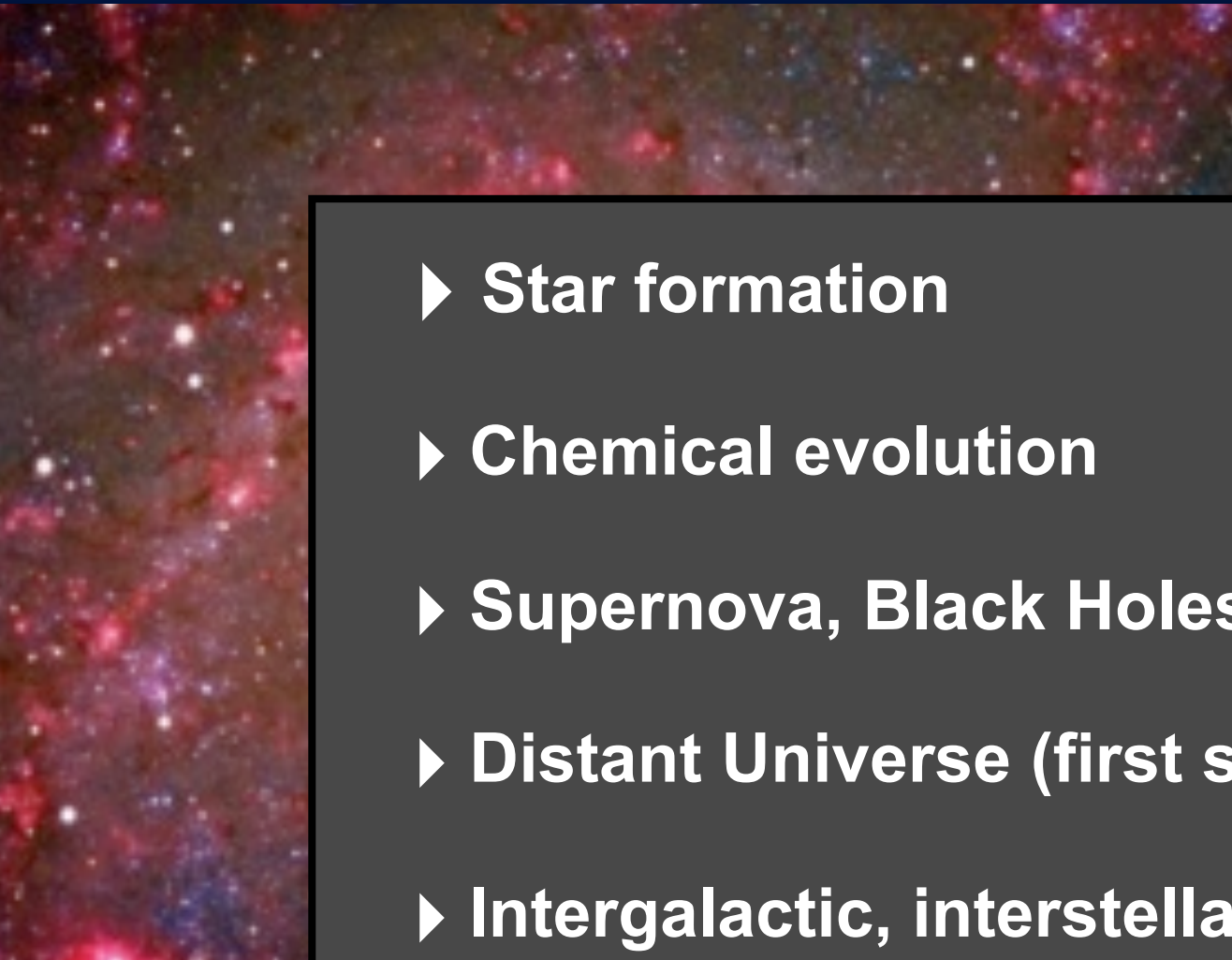
Collaborators

O. Absil (Liege), JP Berger (ESO), M. de Becker (Liege),
JB Le Bouquin (Grenoble), J. Hillier (Pittsburgh), T. Madura (NASA/
GSFC), S. Owocki (Delaware), H. Sana (STScI), G. Weigelt (Bonn)

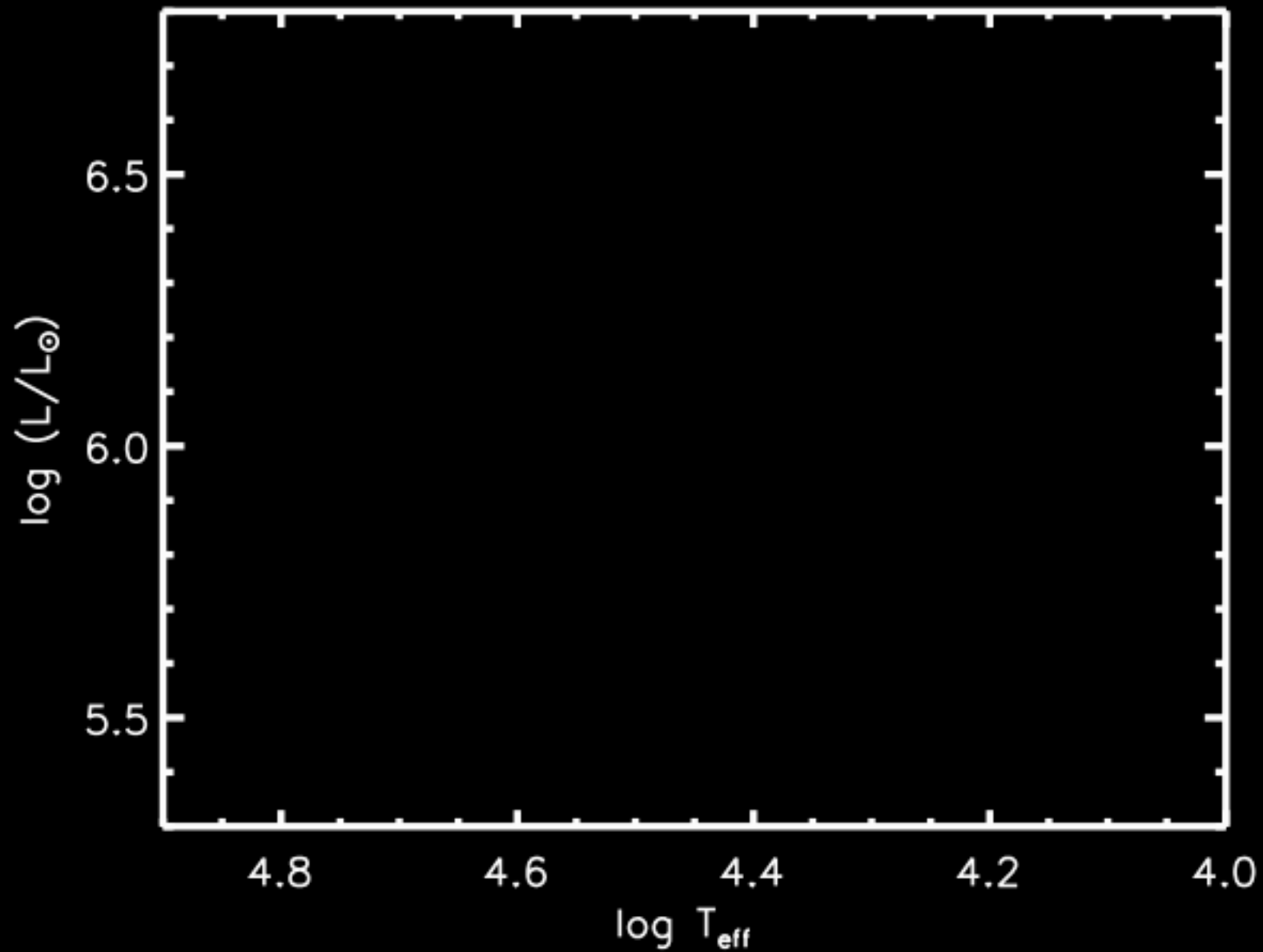


Massive stars bridge many fields of (astro)Physics

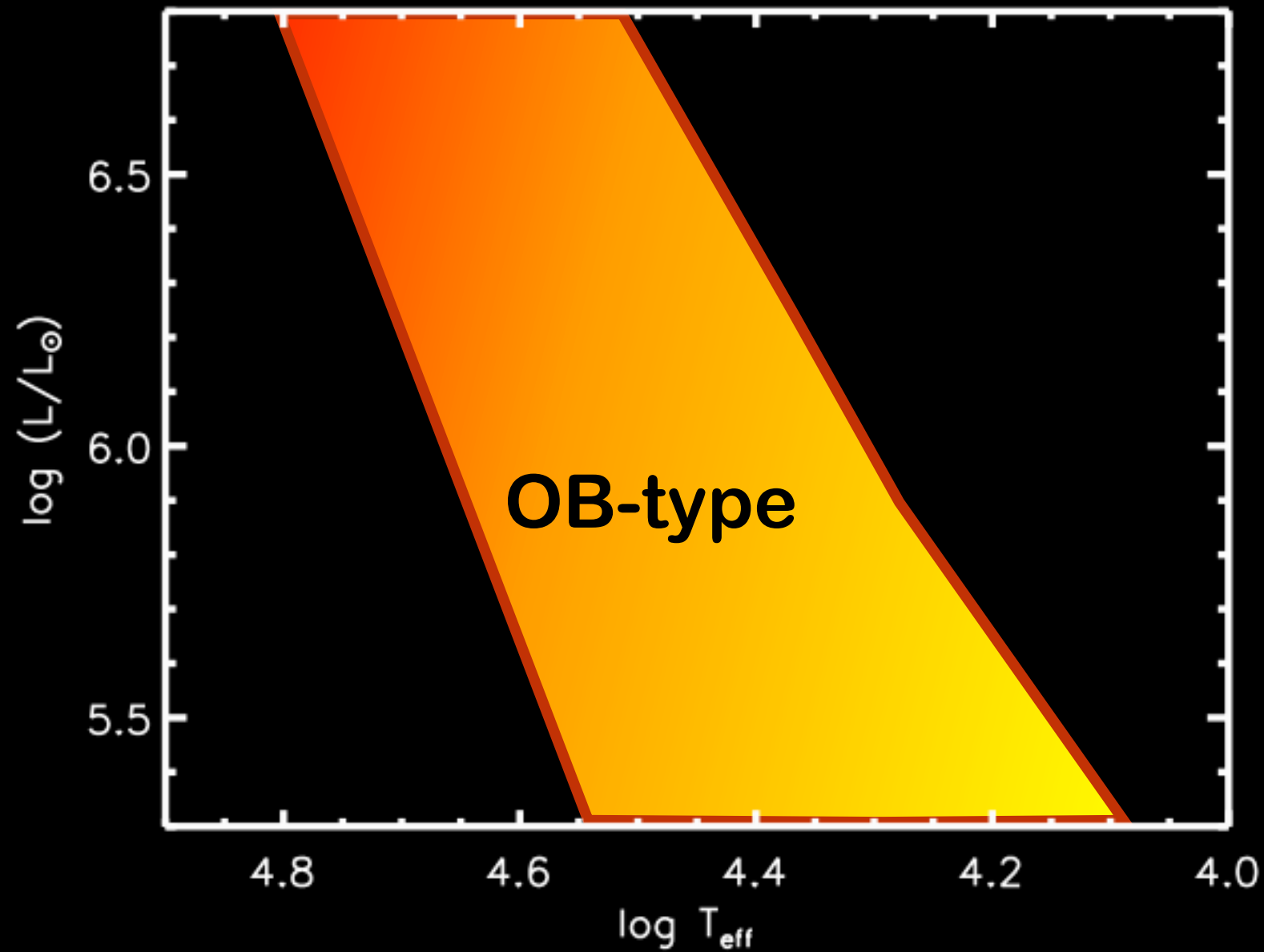
- ▶ Star formation
- ▶ Chemical evolution
- ▶ Supernova, Black Holes, Neutron Stars
- ▶ Distant Universe (first stars, reionization, cosmology)
- ▶ Intergalactic, interstellar, circumstellar media
- ▶ High-energy physics, particle physics, ...
- ▶ **Stellar evolution**



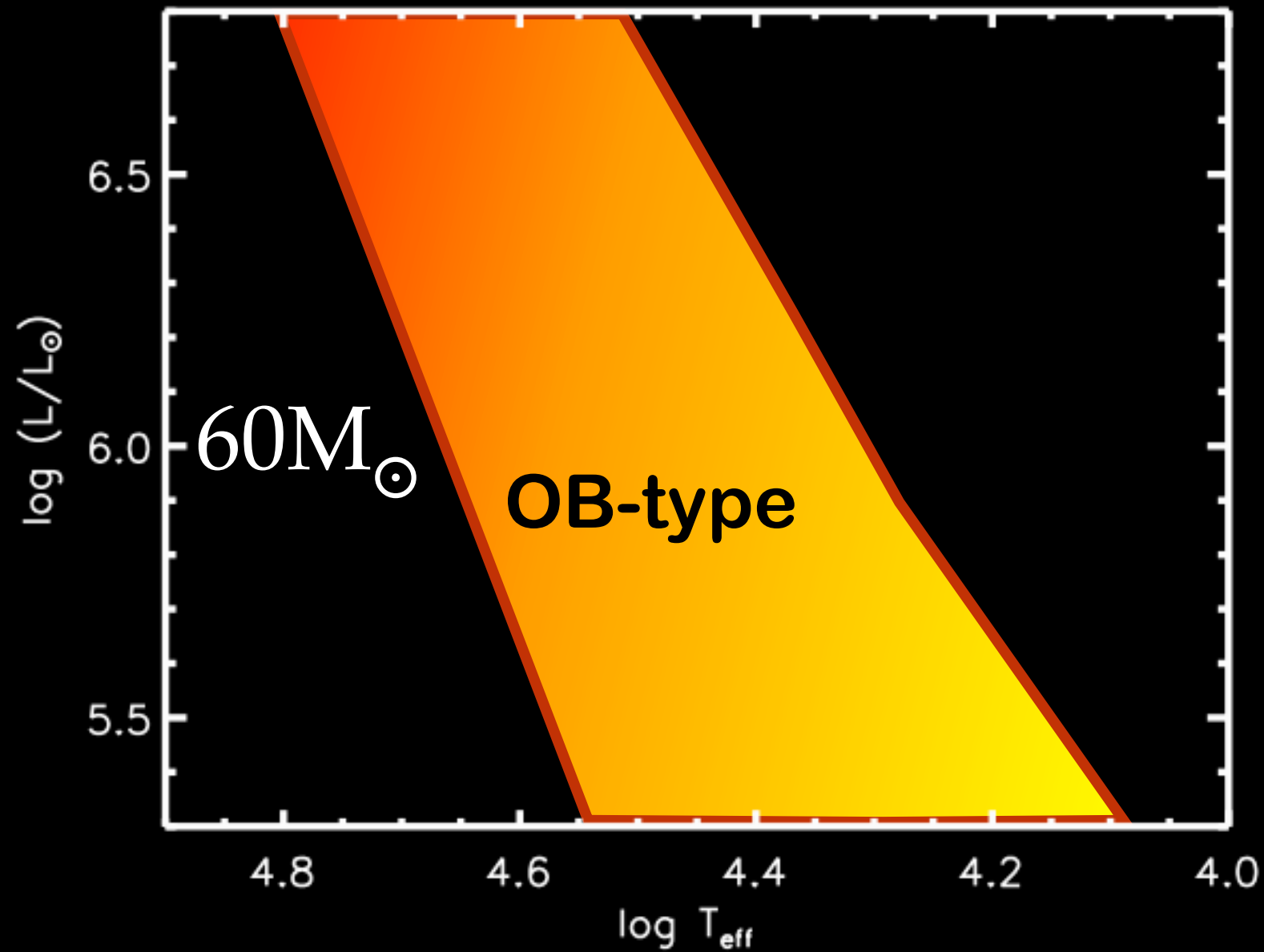
Stellar evolution above $30 M_{\odot}$ at solar Z



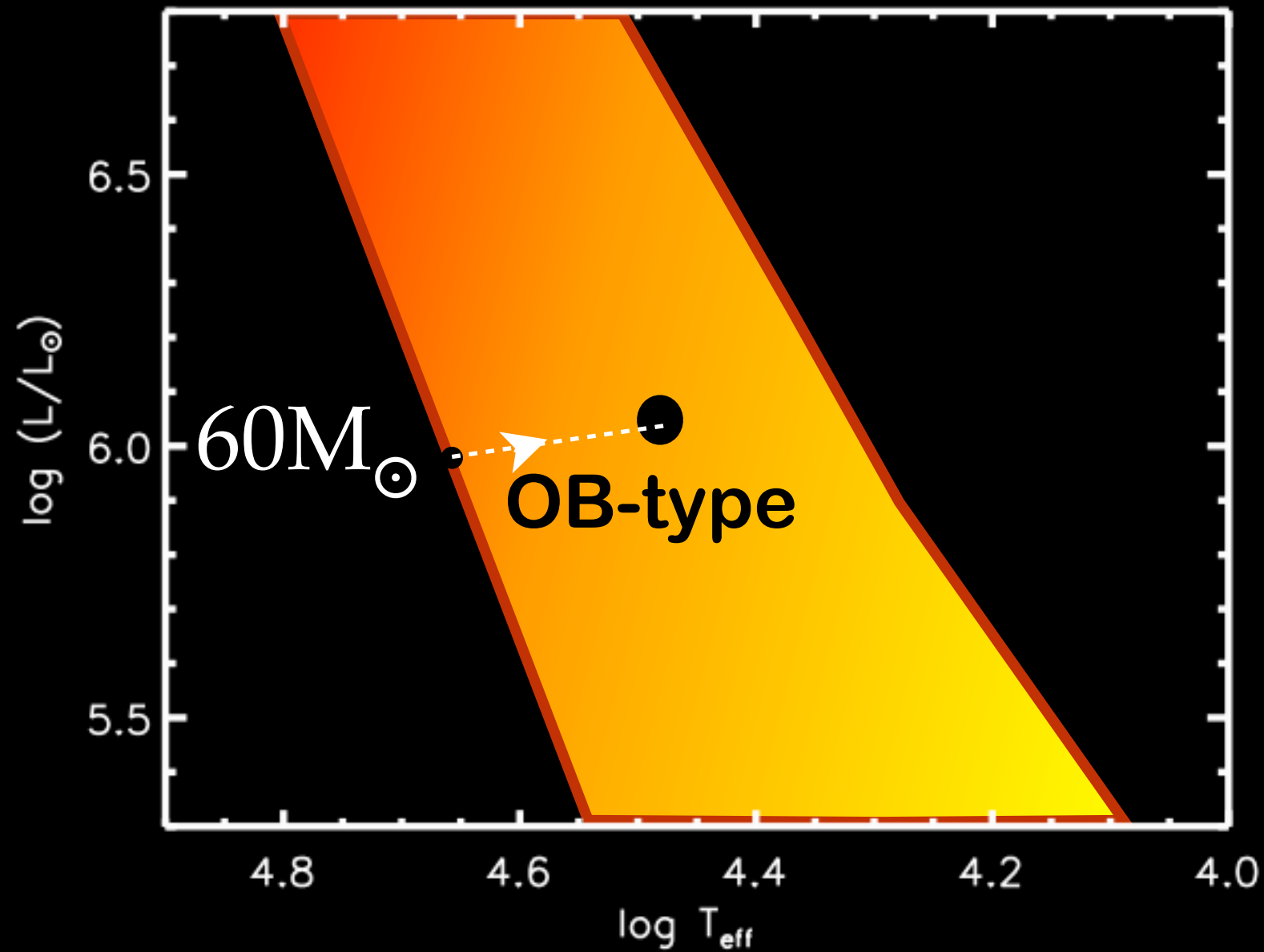
Stellar evolution above $30 M_{\odot}$ at solar Z



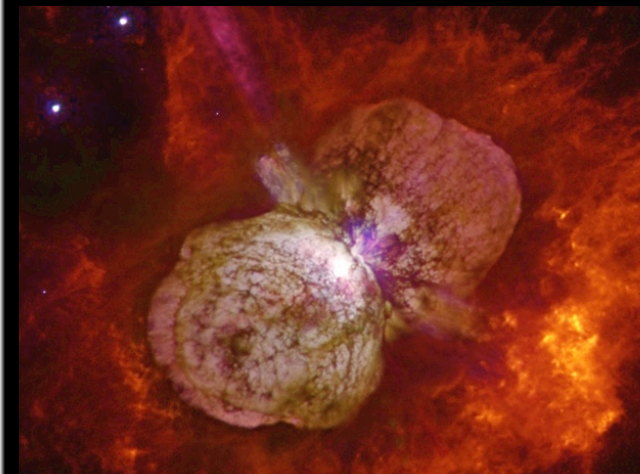
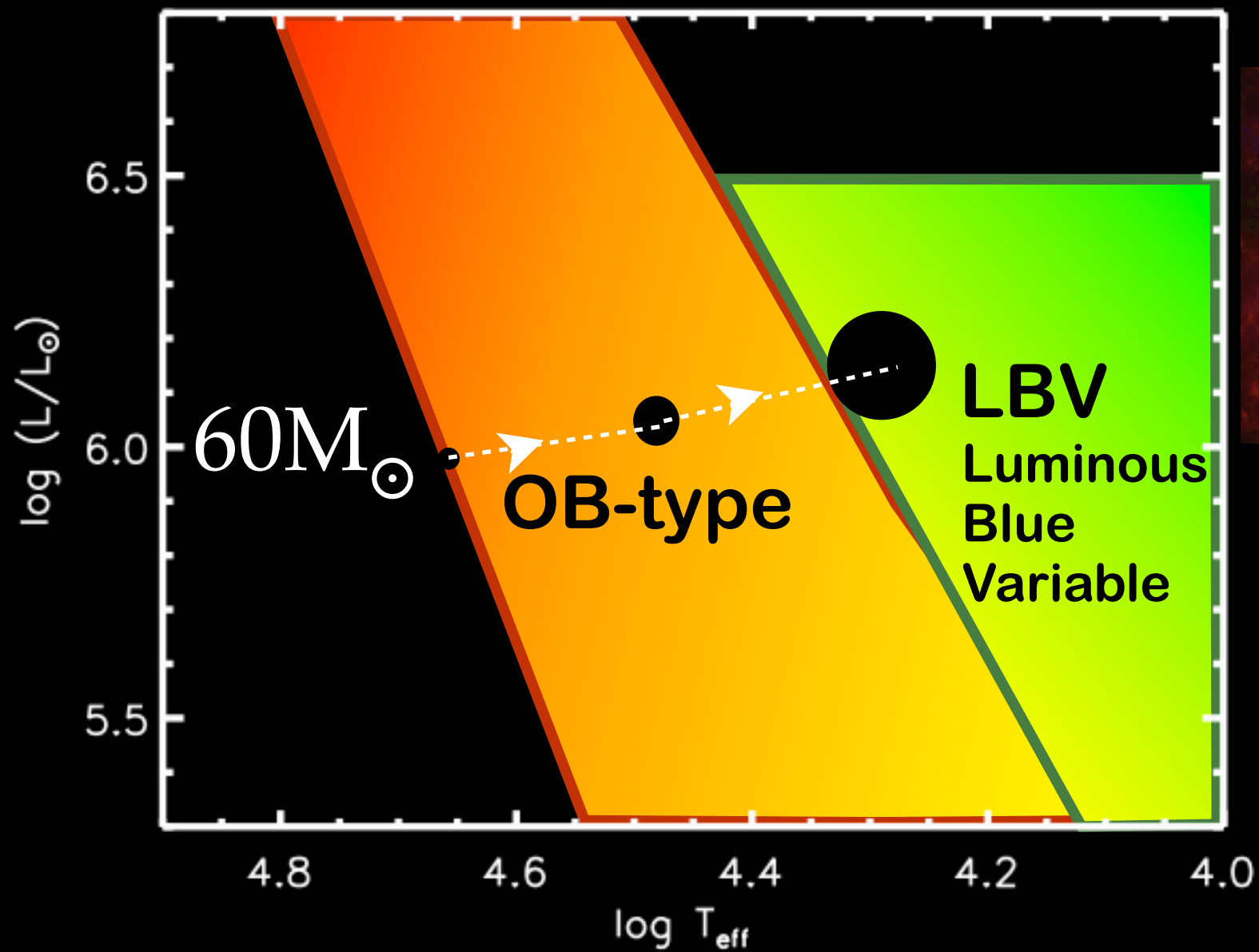
Stellar evolution above $30 M_{\odot}$ at solar Z



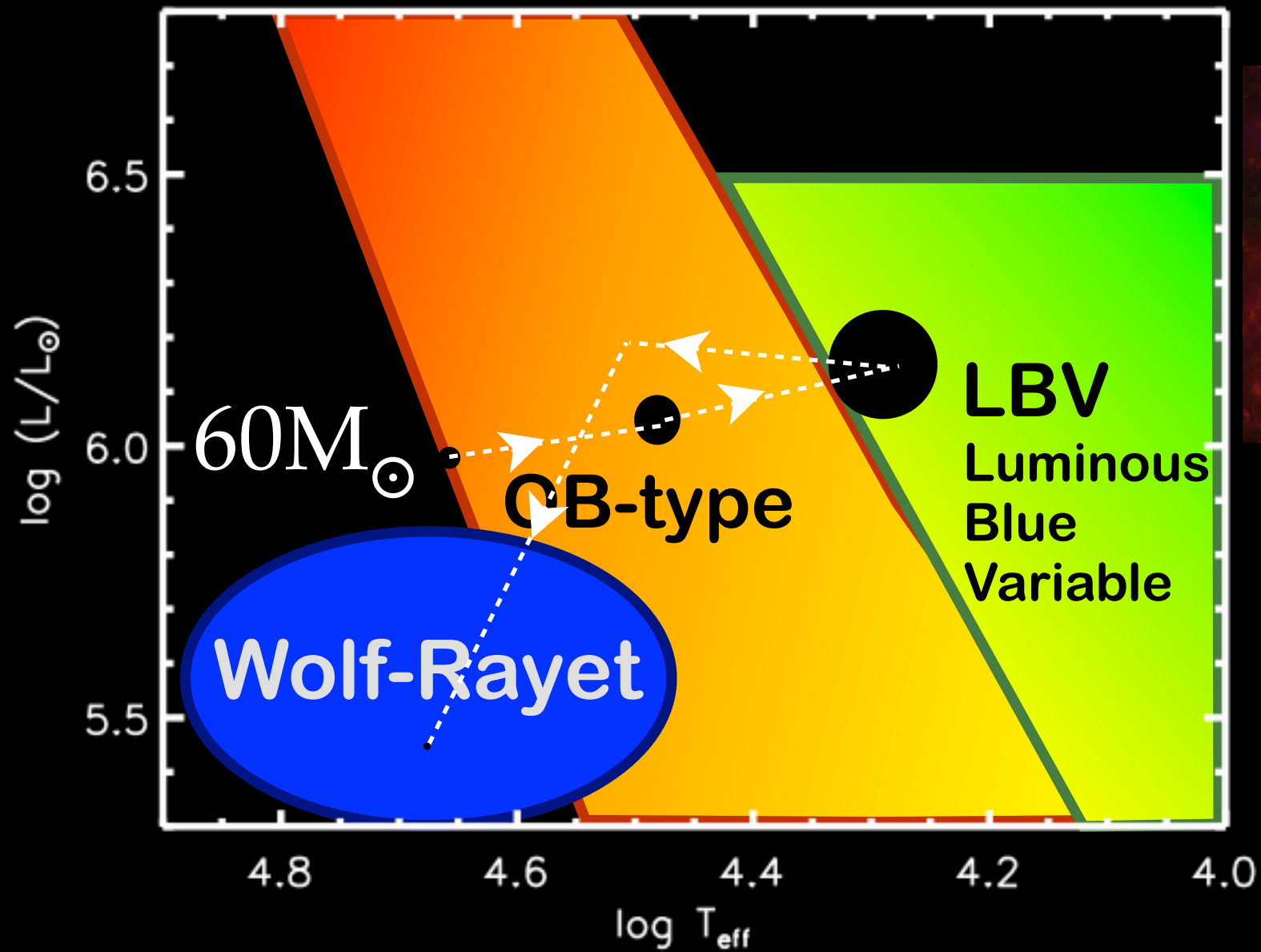
Stellar evolution above $30 M_{\odot}$ at solar Z



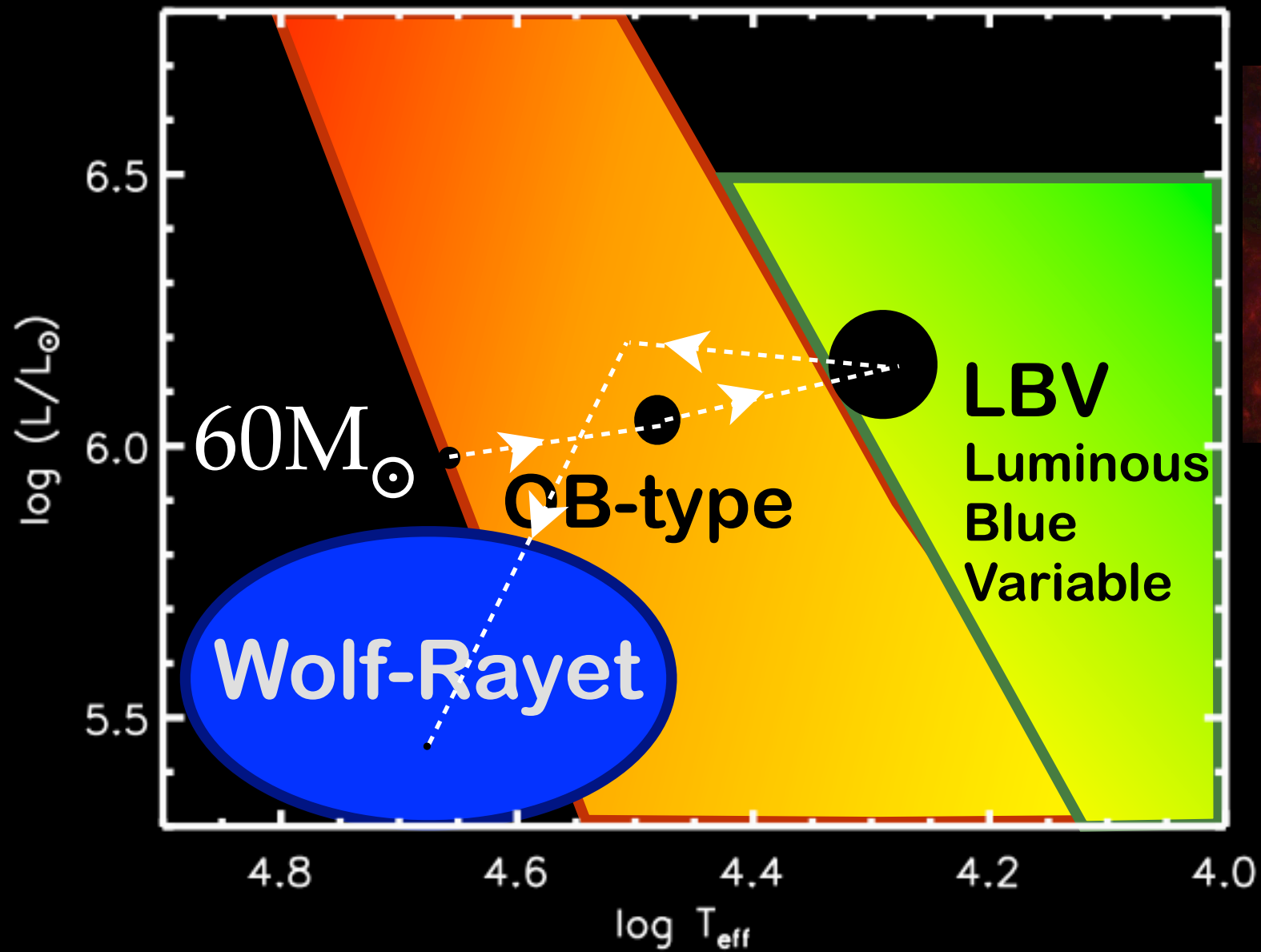
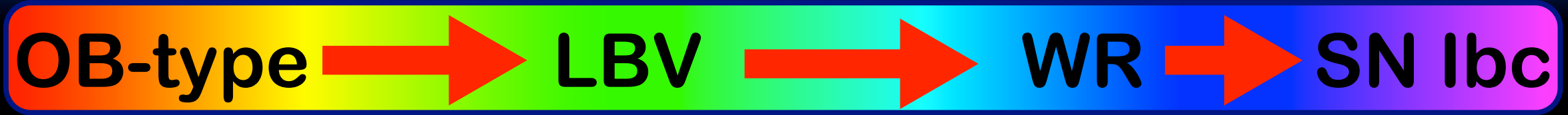
Stellar evolution above $30 M_{\odot}$ at solar Z



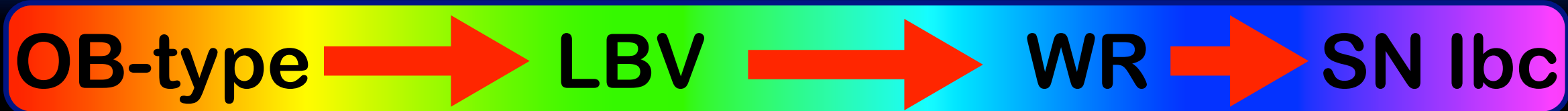
Stellar evolution above $30 M_{\odot}$ at solar Z



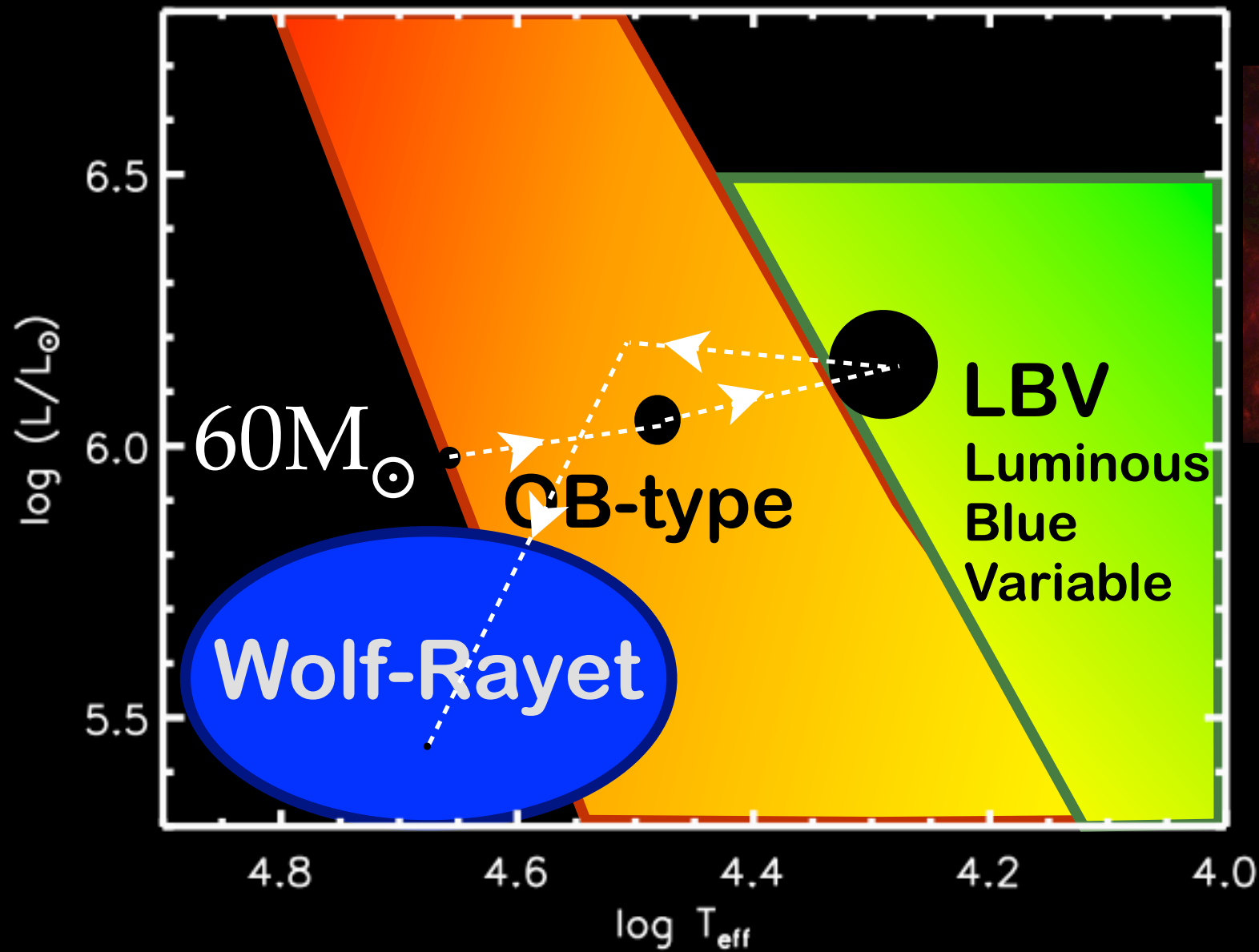
Stellar evolution above $30 M_{\odot}$ at solar Z



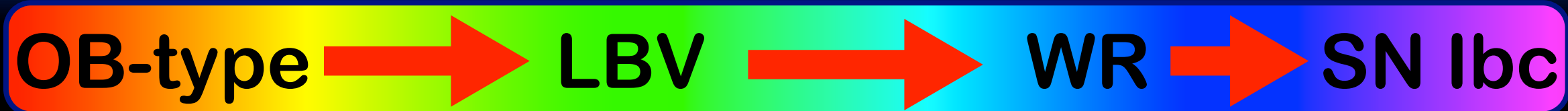
Stellar evolution above $30 M_{\odot}$ at solar Z



LBVs detected as SN progenitors (Kotak & Vink 06; Smith+ 07, 10, 11; Pastorello+ 07; Gal-Yam & Leonard 07, 09; Mauerhan+ 12; Fraser+ 13)

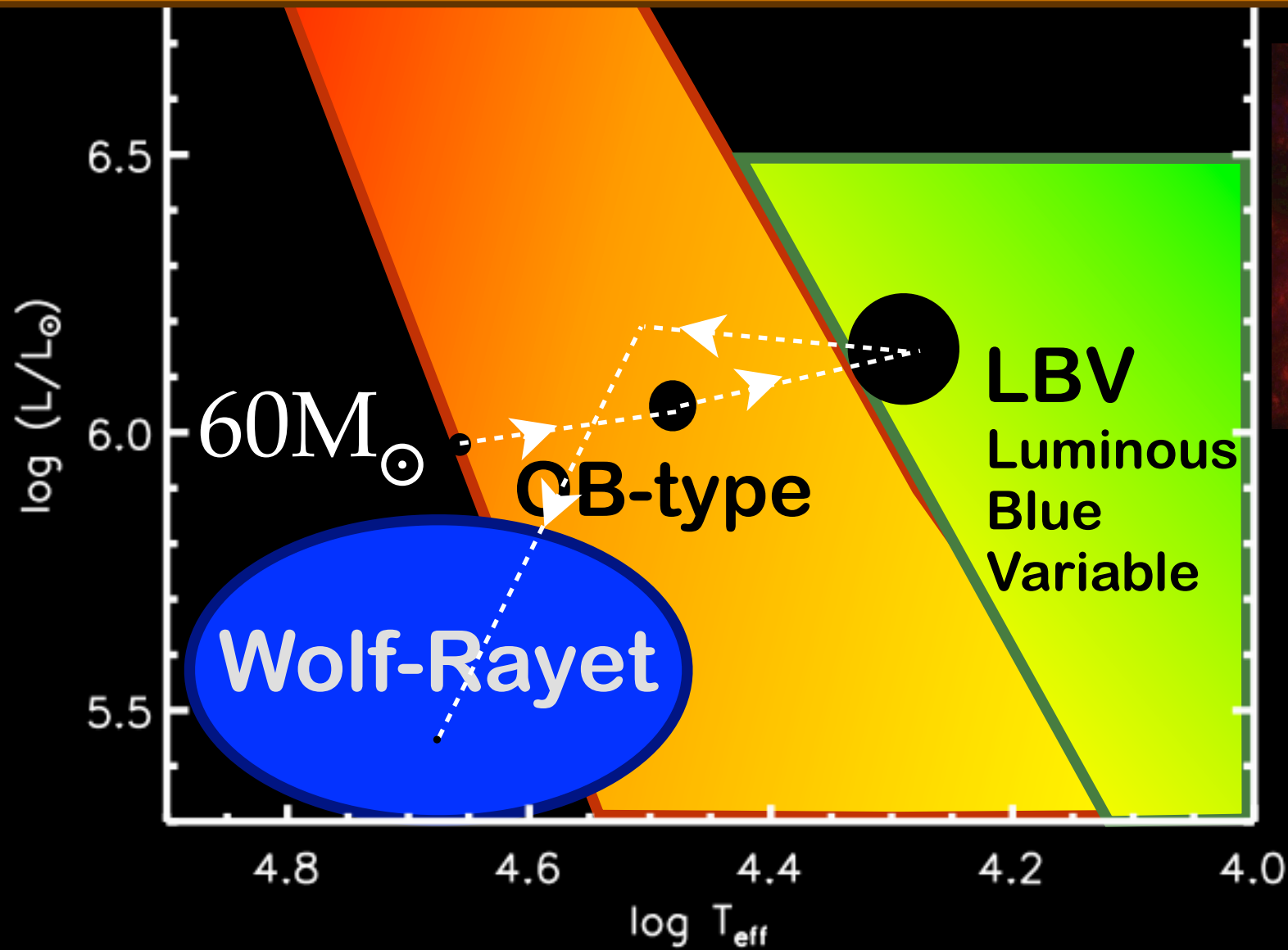


Stellar evolution above 30 M_{\odot} at solar Z

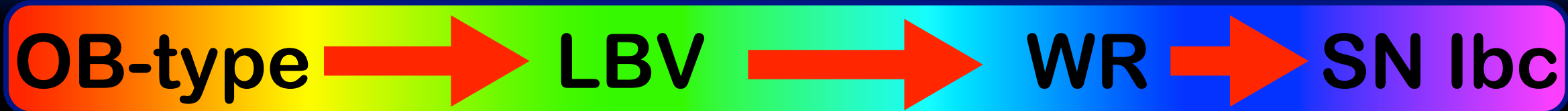


LBVs detected as SN progenitors (Kotak & Vink 06; Smith+ 07, 10, 11; Pastorello+ 07; Gal-Yam & Leonard 07, 09; Mauerhan+ 12; Fraser+ 13)

WRs not detected as SN progenitors? (Maund & Smartt 05; Maund+ 05; Crockett+ 07; Smartt09; Eldridge+ 13; Elias-Rosa+ 13; Bersten+ 14)



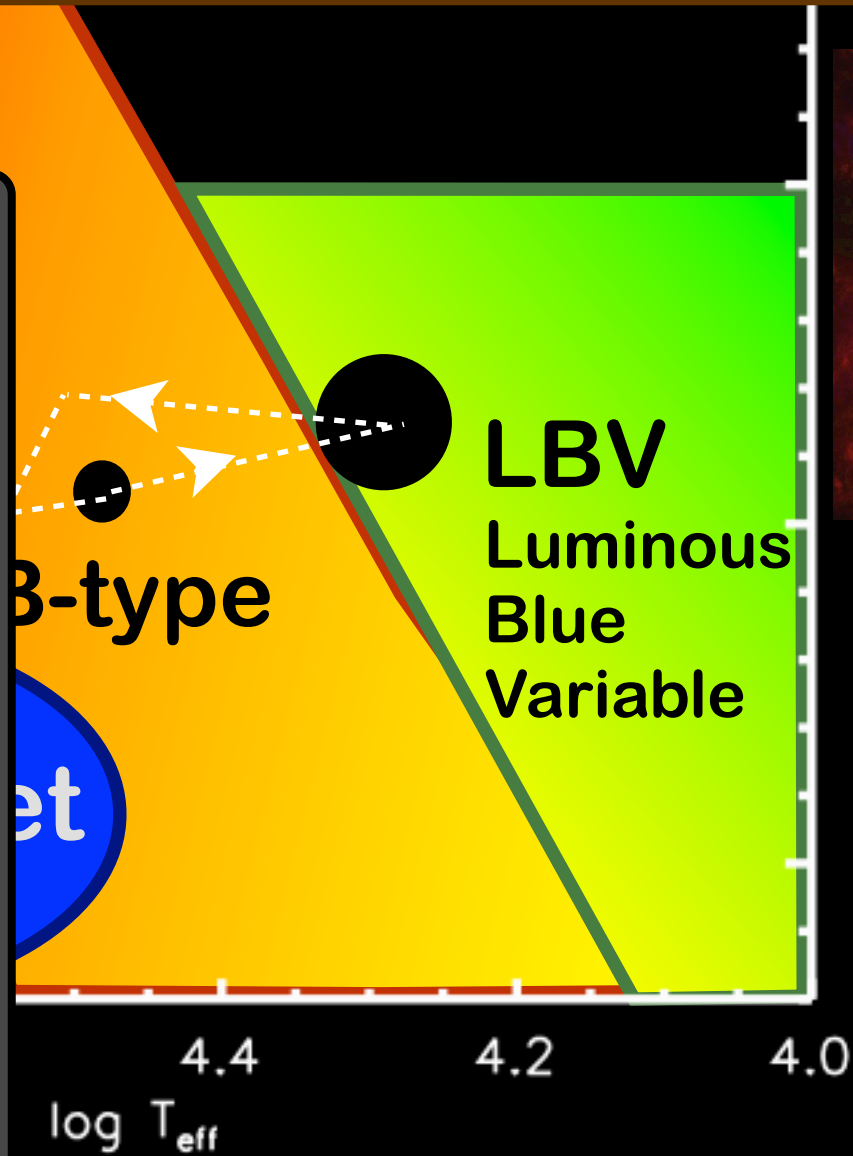
Stellar evolution above $30 M_{\odot}$ at solar Z



LBVs detected as SN progenitors (Kotak & Vink 06; Smith+ 07, 10, 11; Pastorello+ 07; Gal-Yam & Leonard 07, 09; Mauerhan+ 12; Fraser+ 13)

WRs not detected as SN progenitors? (Maund & Smartt 05; Maund+ 05; Crockett+ 07; Smartt09; Eldridge+ 13; Elias-Rosa+ 13; Bersten+ 14)

- ▶ **Binarity**
- ▶ **Mass loss and eruptions**
- ▶ **Rotation**
- ▶ **Magnetic Fields**
- ▶ **Convection**
- ▶ **Going from 3D to 1D**
- ▶ **Metallicity**
- ▶ **Explosion properties,**



Eta Carinae and the Homunculus nebula



Central Source:

$$L \sim 5 \times 10^6 L_{\odot}$$

$$M > 150 M_{\odot}$$

$$\dot{M} \sim 8 \times 10^{-4} M_{\odot}/\text{yr}$$

$$v_{\text{inf}} \sim 420 \text{ km/s}$$

(Hillier+ 01, Groh+ 12)

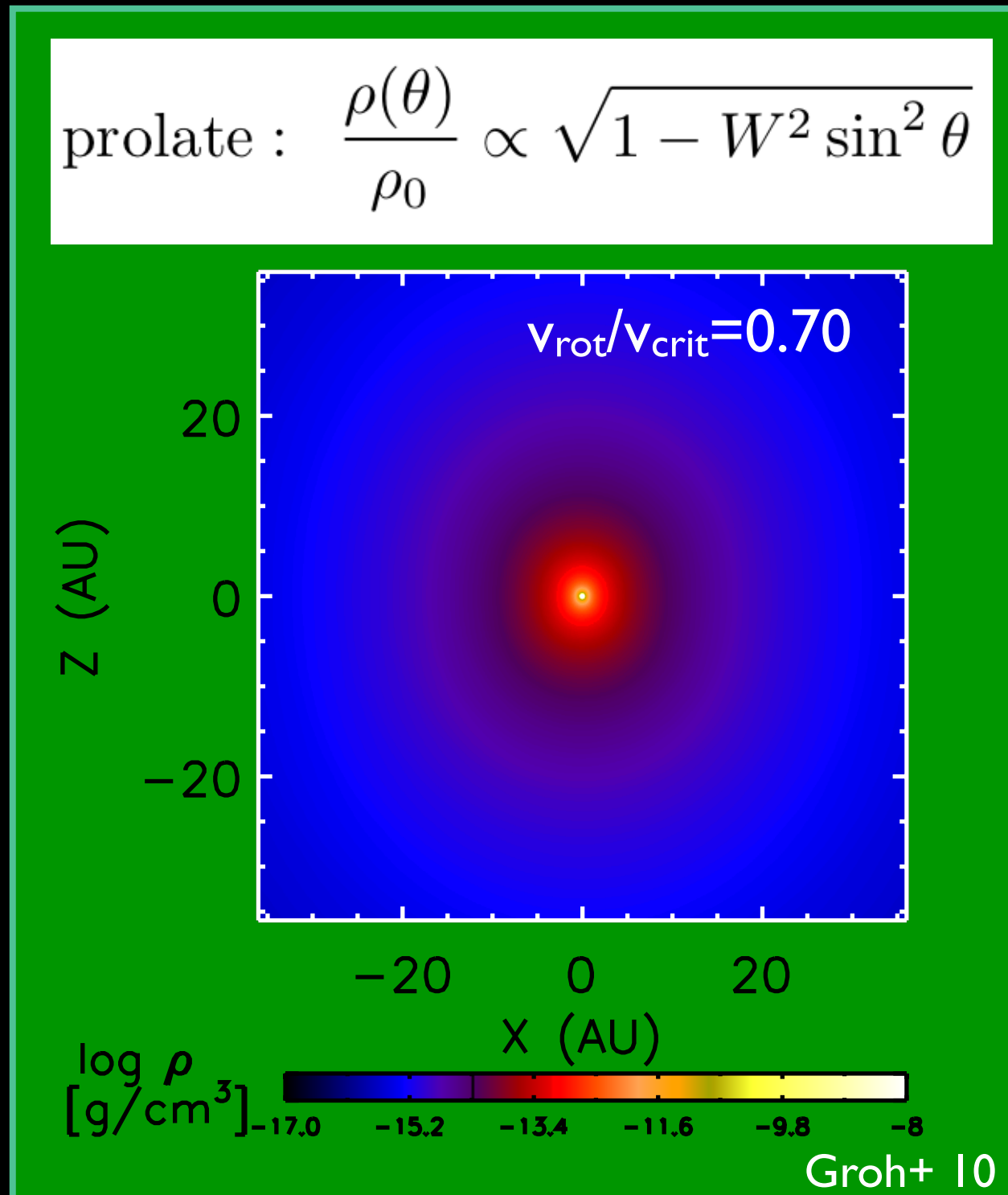
Needs interferometry to probe the inner 10 mas:

- rotation
- mass loss
- binarity

Effects of rapid rotation on a stellar wind

Deviation from spherical symmetry depends on $W=v_{\text{rot}}/v_{\text{crit}}$ (Owocki et al. 1998):

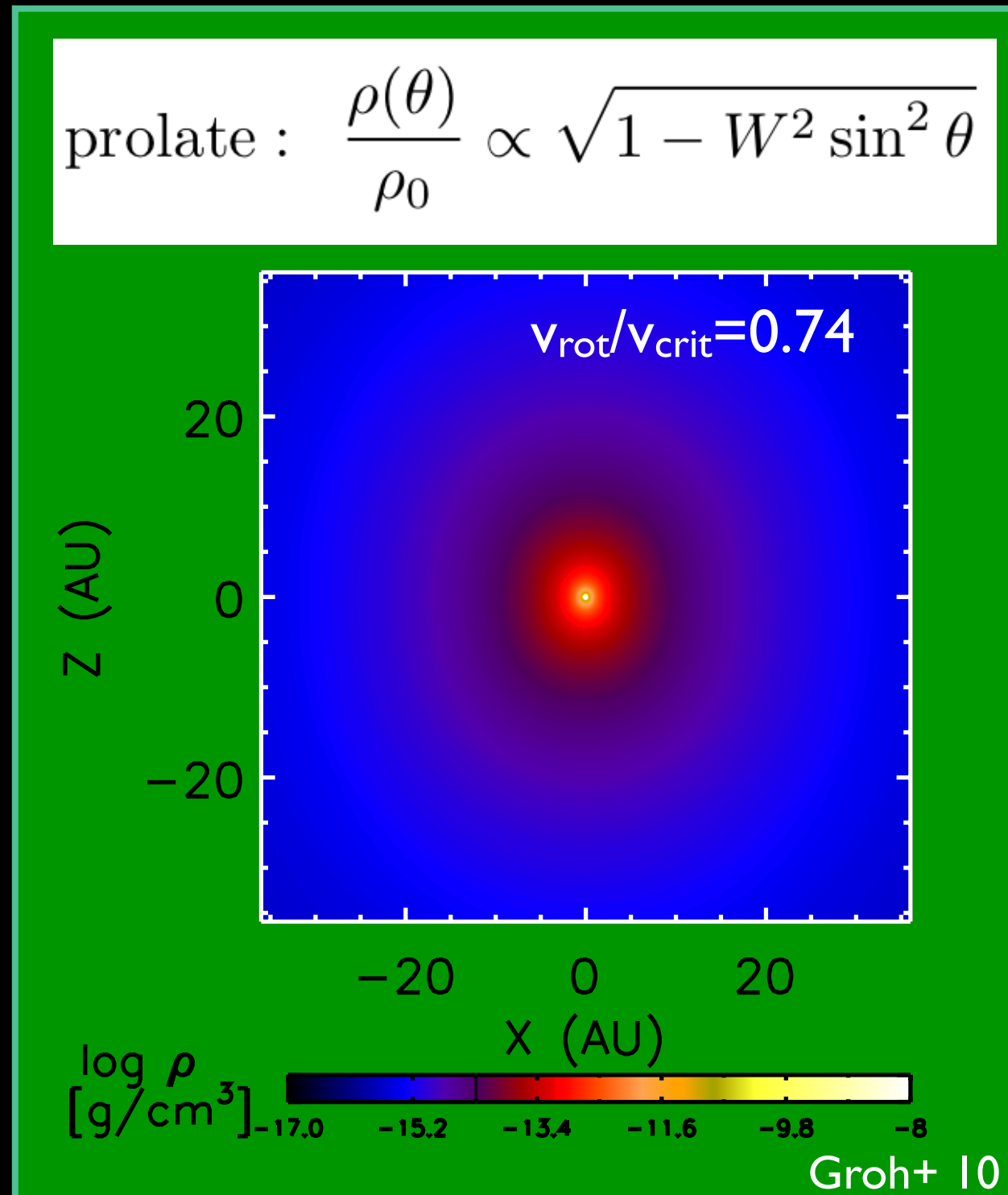
$$\text{prolate : } \frac{\rho(\theta)}{\rho_0} \propto \sqrt{1 - W^2 \sin^2 \theta}$$



Effects of rapid rotation on a stellar wind

Deviation from spherical symmetry depends on $W = v_{\text{rot}}/v_{\text{crit}}$ (Owocki et al. 1998):

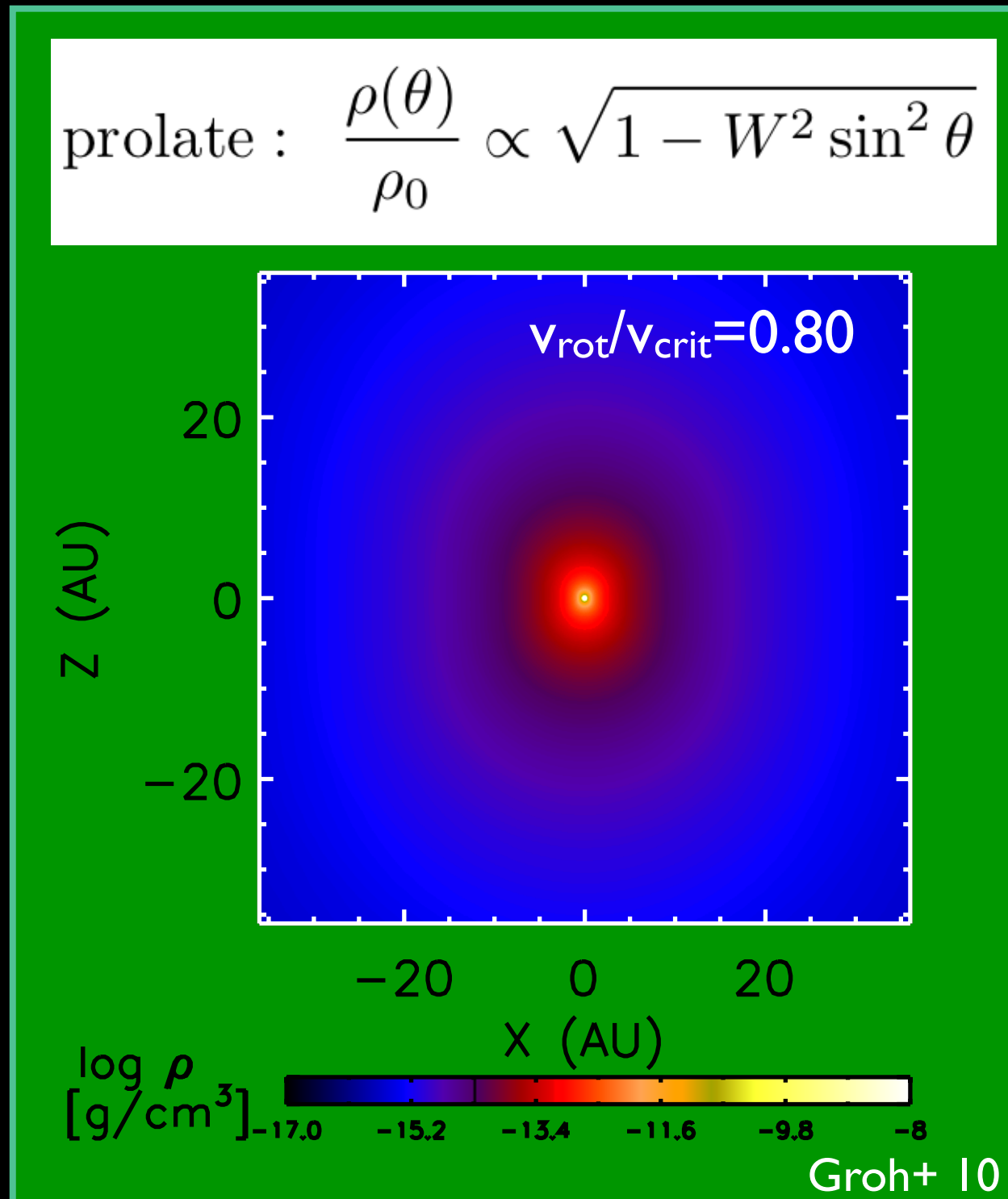
$$\text{prolate : } \frac{\rho(\theta)}{\rho_0} \propto \sqrt{1 - W^2 \sin^2 \theta}$$



Effects of rapid rotation on a stellar wind

Deviation from spherical symmetry depends on $W = v_{\text{rot}}/v_{\text{crit}}$ (Owocki et al. 1998):

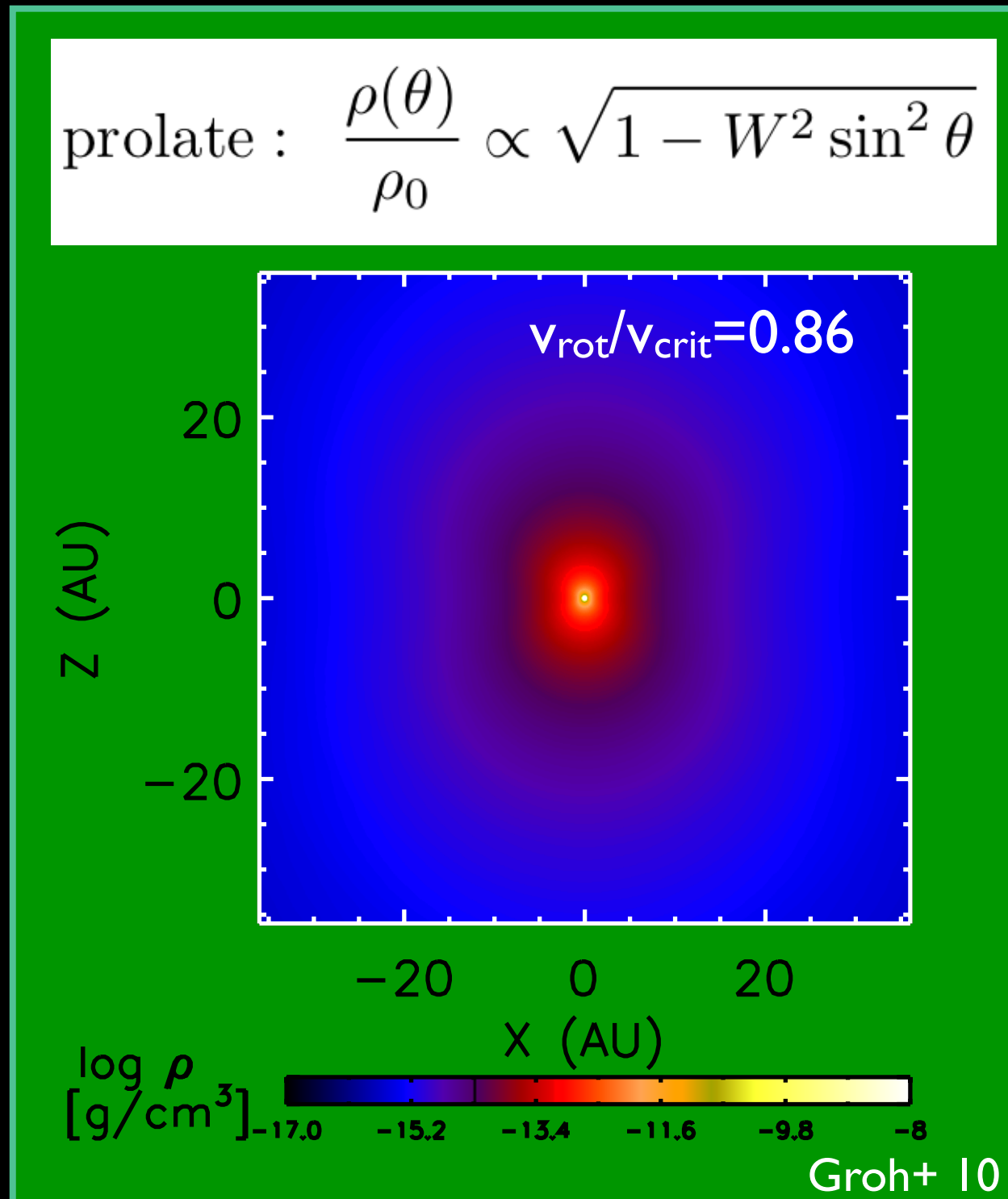
$$\text{prolate : } \frac{\rho(\theta)}{\rho_0} \propto \sqrt{1 - W^2 \sin^2 \theta}$$



Effects of rapid rotation on a stellar wind

Deviation from spherical symmetry depends on $W = v_{\text{rot}}/v_{\text{crit}}$ (Owocki et al. 1998):

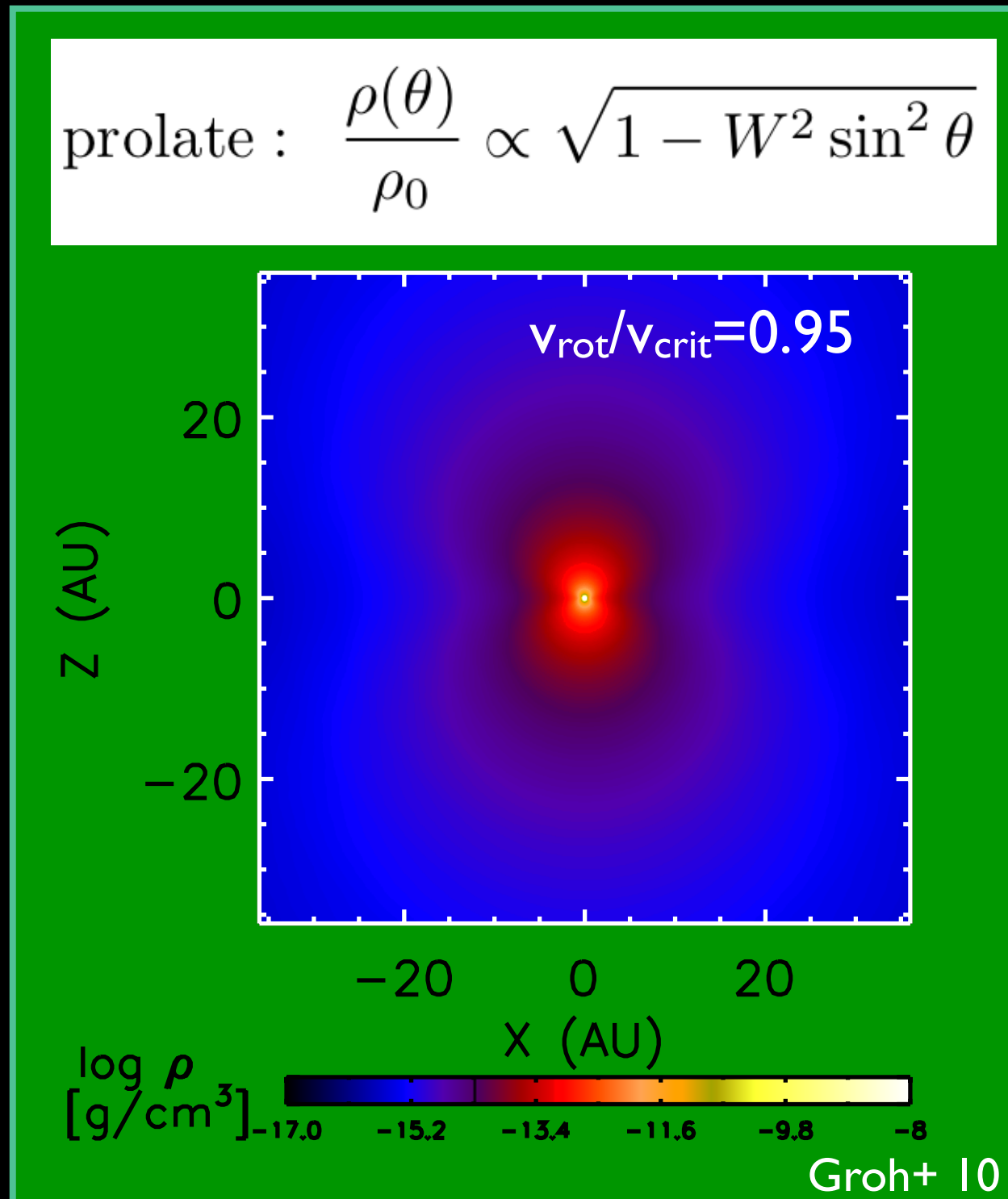
$$\text{prolate : } \frac{\rho(\theta)}{\rho_0} \propto \sqrt{1 - W^2 \sin^2 \theta}$$



Effects of rapid rotation on a stellar wind

Deviation from spherical symmetry depends on $W = v_{\text{rot}}/v_{\text{crit}}$ (Owocki et al. 1998):

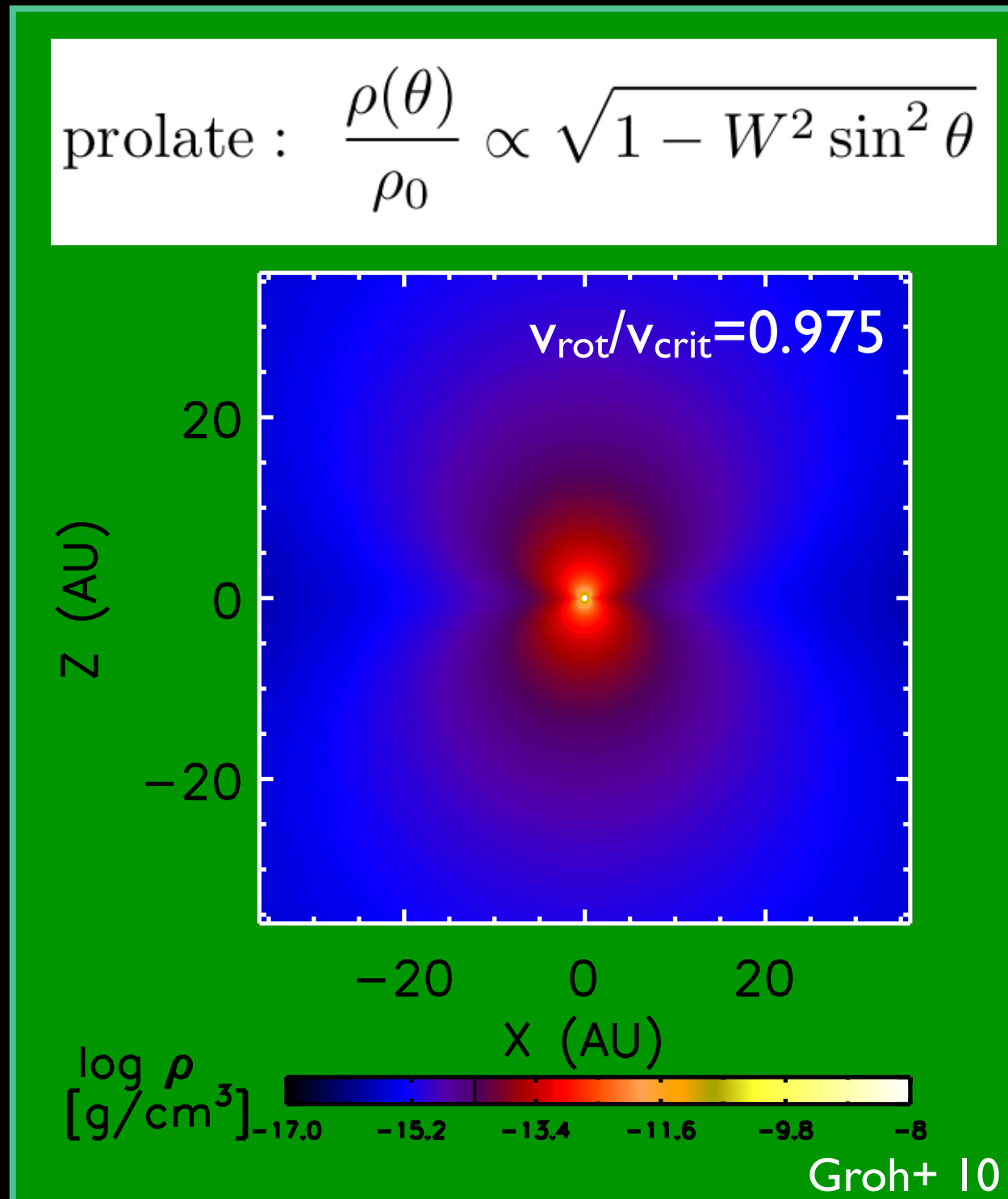
$$\text{prolate : } \frac{\rho(\theta)}{\rho_0} \propto \sqrt{1 - W^2 \sin^2 \theta}$$



Effects of rapid rotation on a stellar wind

Deviation from spherical symmetry depends on $W = v_{\text{rot}}/v_{\text{crit}}$ (Owocki et al. 1998):

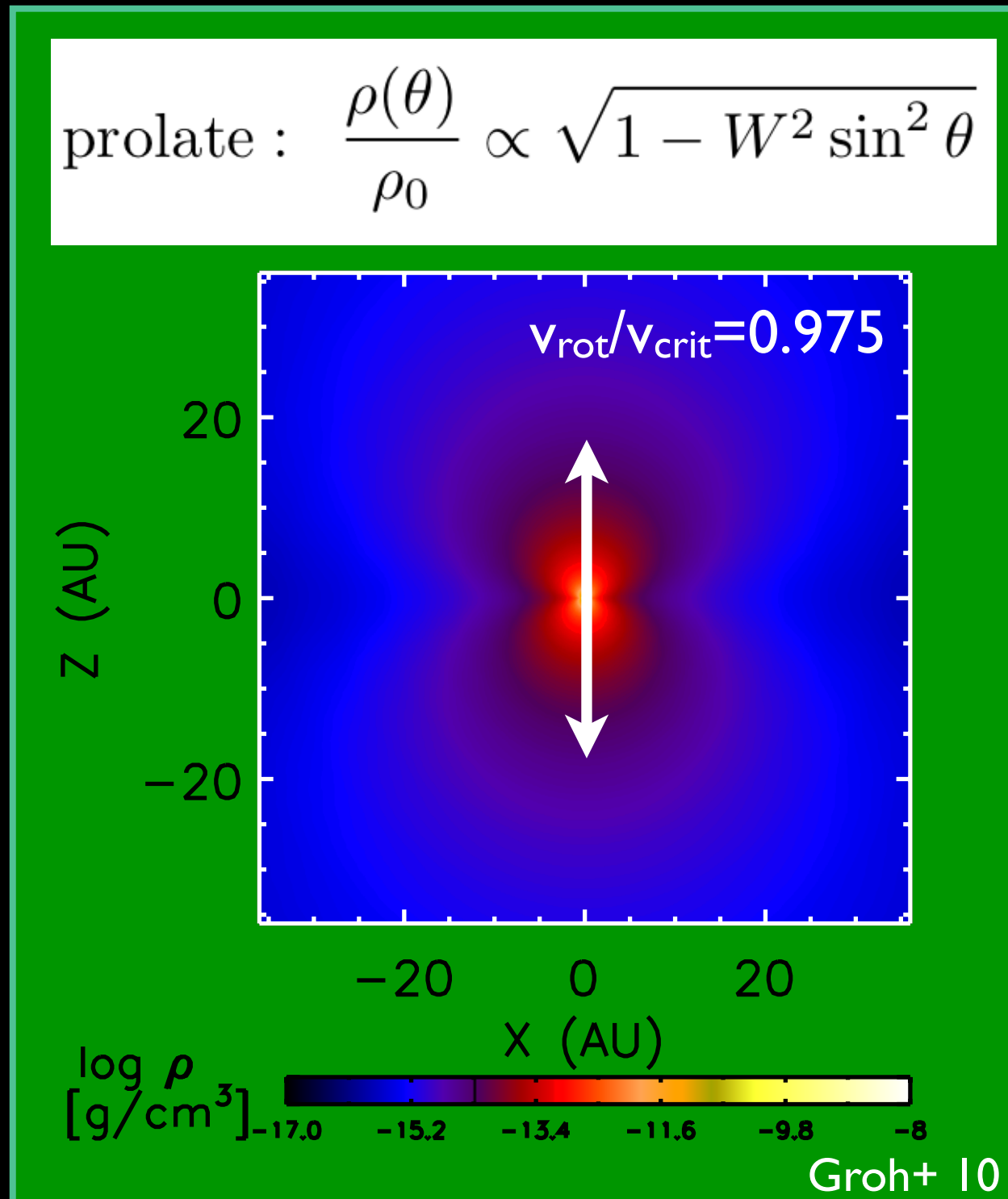
$$\text{prolate : } \frac{\rho(\theta)}{\rho_0} \propto \sqrt{1 - W^2 \sin^2 \theta}$$



Effects of rapid rotation on a stellar wind

Deviation from spherical symmetry depends on $W = v_{\text{rot}}/v_{\text{crit}}$ (Owocki et al. 1998):

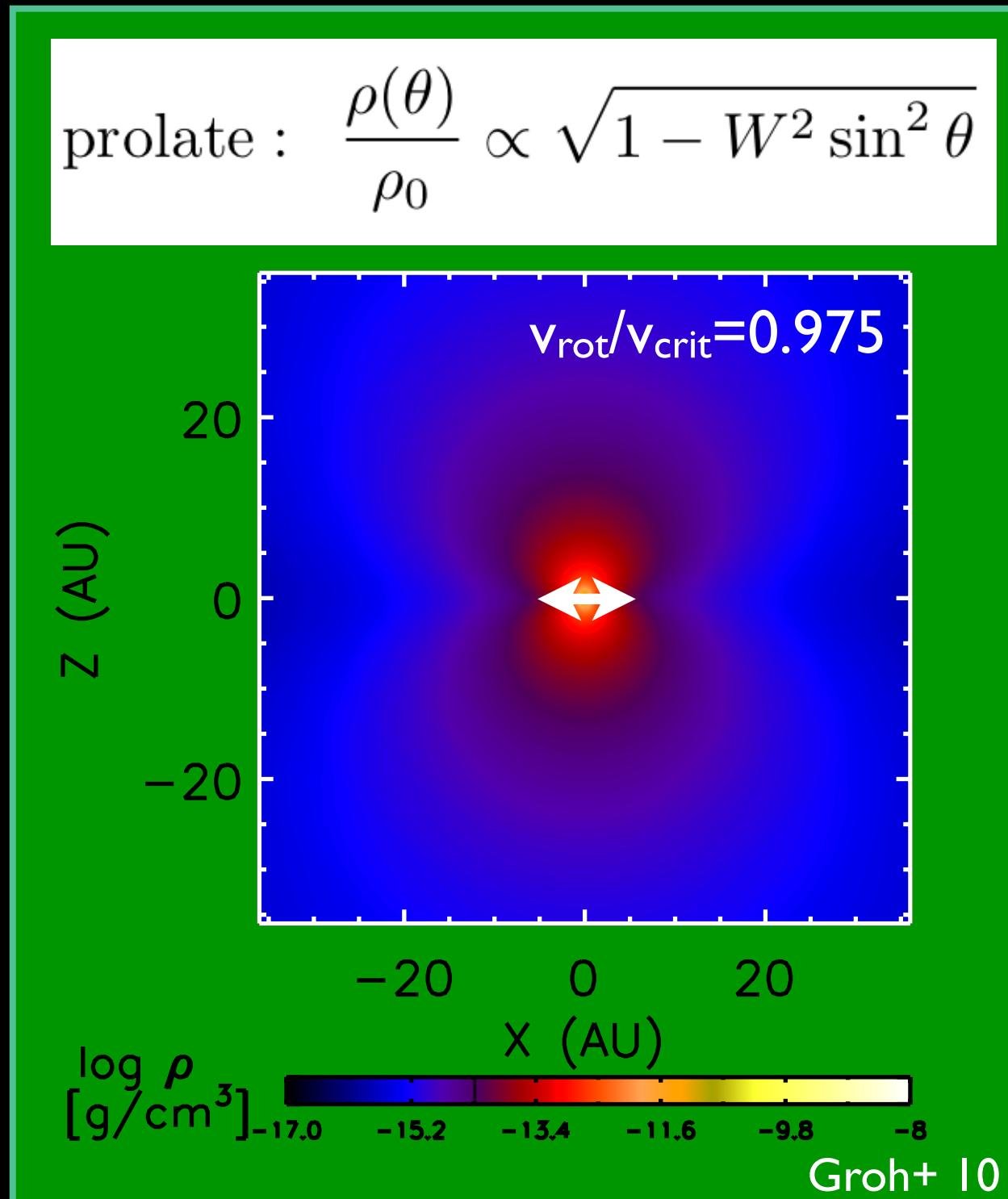
$$\text{prolate : } \frac{\rho(\theta)}{\rho_0} \propto \sqrt{1 - W^2 \sin^2 \theta}$$



Effects of rapid rotation on a stellar wind

Deviation from spherical symmetry depends on $W = v_{\text{rot}}/v_{\text{crit}}$ (Owocki et al. 1998):

$$\text{prolate : } \frac{\rho(\theta)}{\rho_0} \propto \sqrt{1 - W^2 \sin^2 \theta}$$



Rotation: elongation of the K-band photosphere

(van Boekel+ 03; Kervella 07; Weigelt+07; Groh+10)

VLTI/VINCI beam-combination instrument
Visibilities in the K-band continuum
Two 0.35-m siderostats using 24m baseline



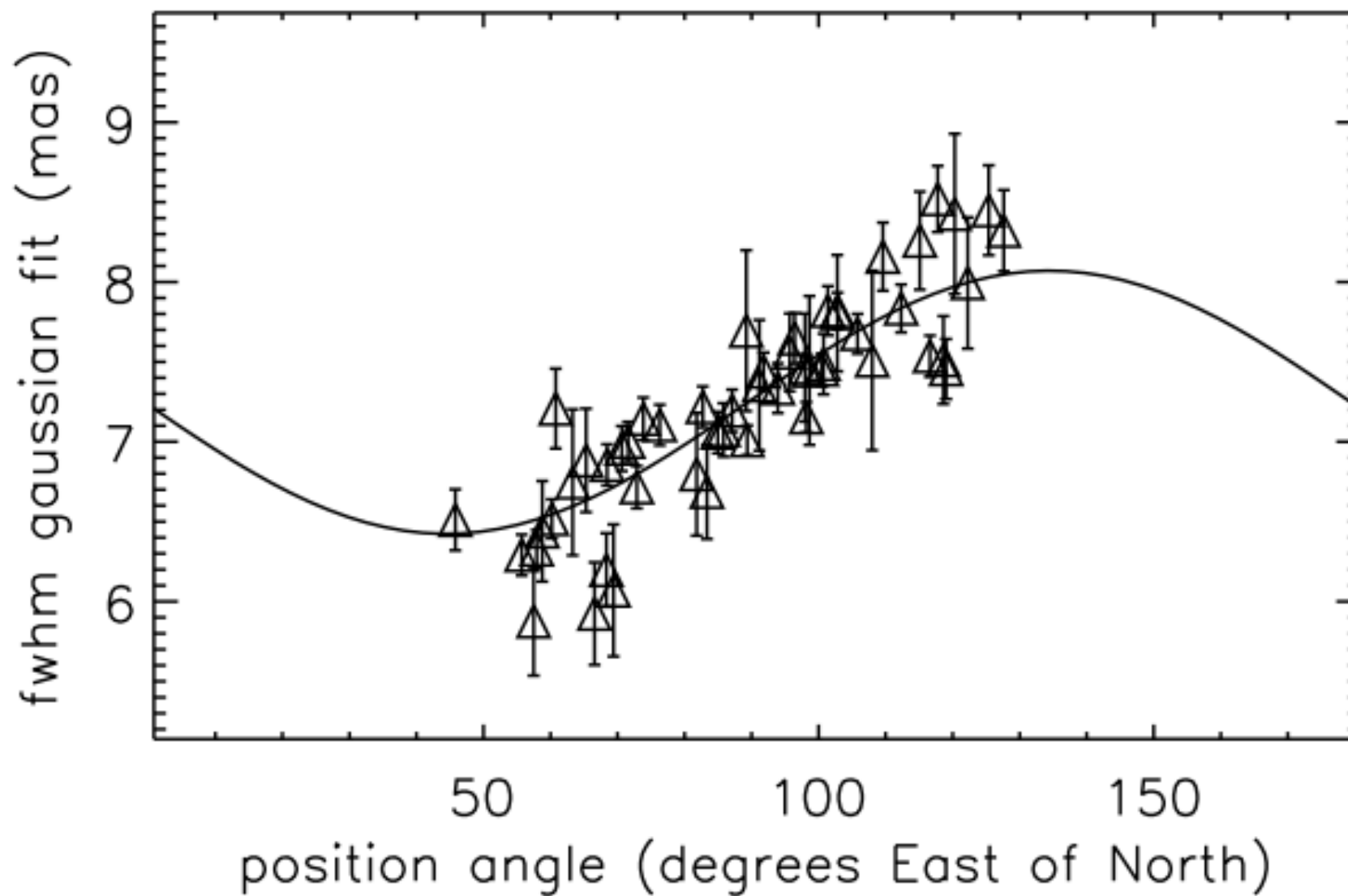
Rotation: elongation of the K-band photosphere

(van Boekel+ 03; Kervella 07; Weigelt+07; Groh+10)

VLT/VINCI beam-combination instrument

Visibilities in the K-band continuum

Two 0.35-m siderostats using 24m baseline



Rotation: elongation of the K-band photosphere

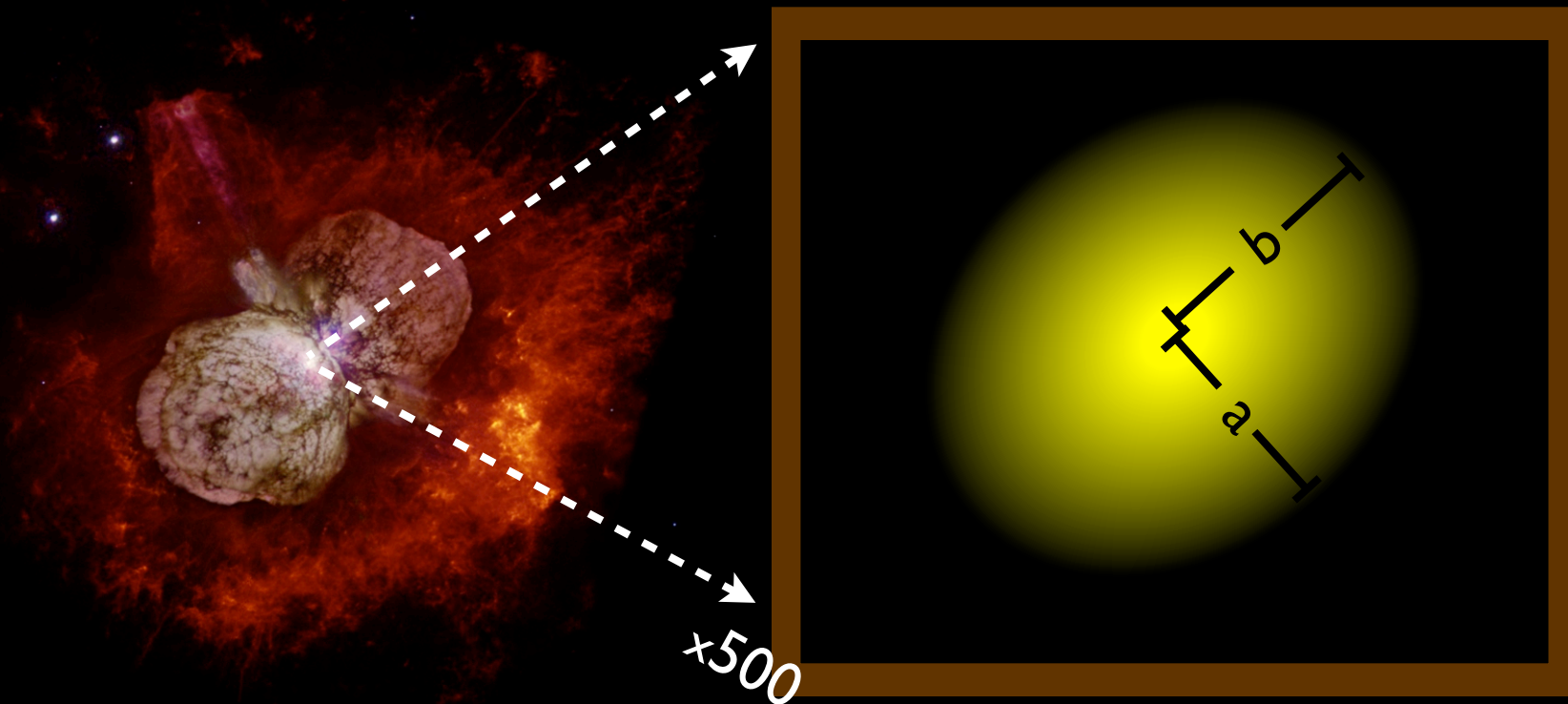
(van Boekel+ 03; Kervella 07; Weigelt+07; Groh+10)

Homunculus

$i=41^\circ$; $PA=131^\circ$

Geometric model

$PA\sim 134^\circ$; $b/a=1.25$



Eta Car A

rapid rotator: rot. axis aligned with the Homunculus polar axis

Rotation: elongation of the K-band photosphere

(van Boekel+ 03; Kervella 07; Weigelt+07; Groh+10)

Homunculus

$i=41^\circ$; $PA=131^\circ$

Geometric model

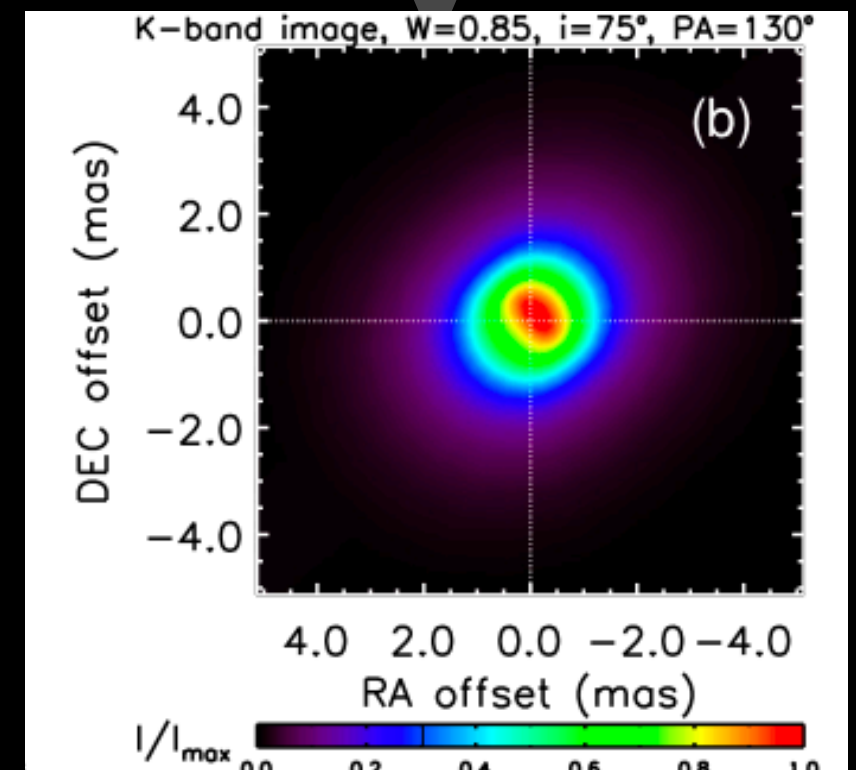
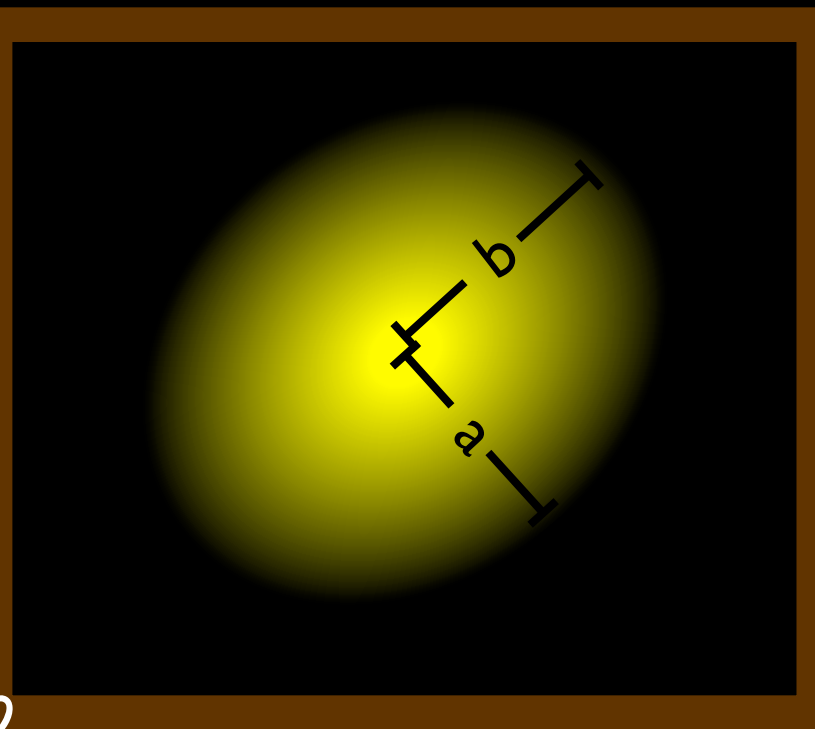
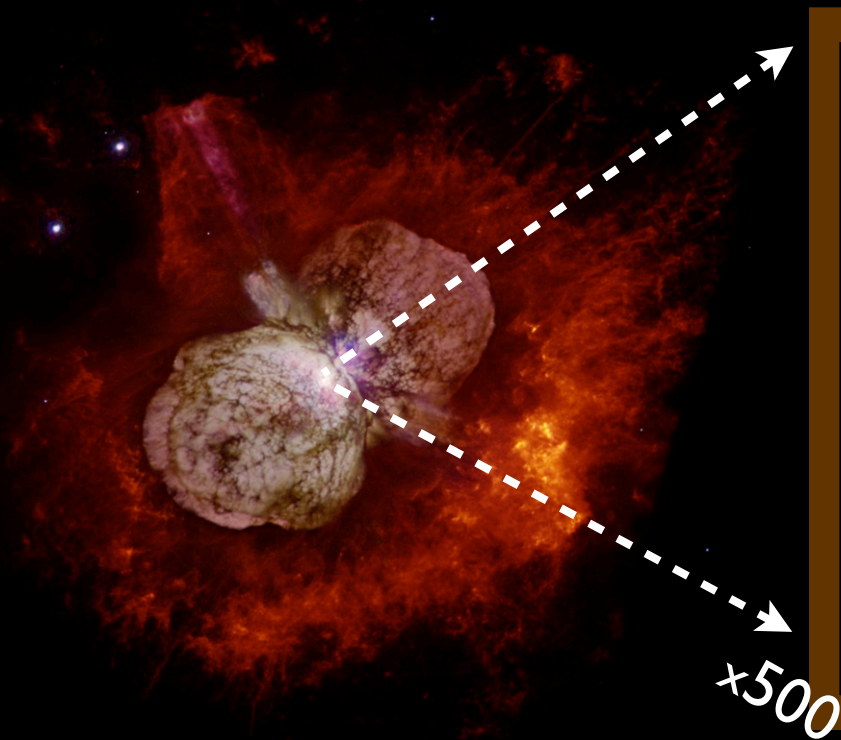
$PA \sim 134^\circ$; $b/a=1.25$

Rad. Transf. VINCI+AMBER

$v_{\text{rot}}/v_{\text{crit}}=0.77$ to 0.92

$i=60^\circ$ to 90°

$PA=108^\circ$ to 142°



Eta Car A

rapid rotator: rot. axis aligned with the Homunculus polar axis

Eta Car A

rapid rotator: rotation axis **misaligned** with the Homunculus

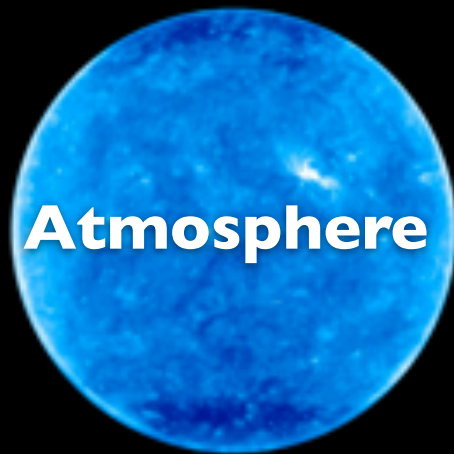
Groh+10

Mass loss and extension of the photosphere

Strong stellar wind causes the photosphere to be formed in the wind

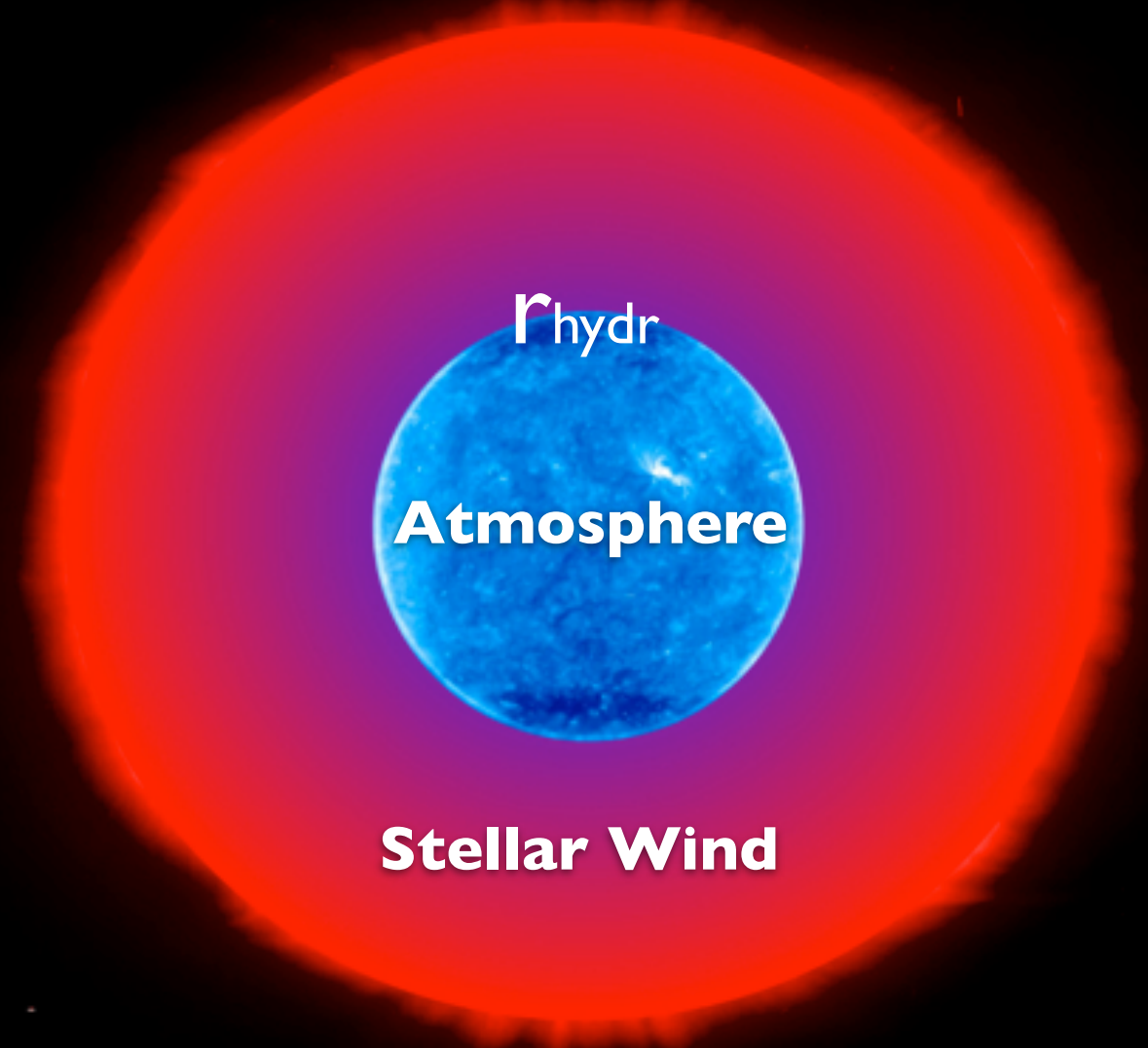
Sun

$r_{\text{hydrostatic}} = r_{\text{photosphere}}$



Eta Car

r_{phot} (set by free-free emission in the K-band)

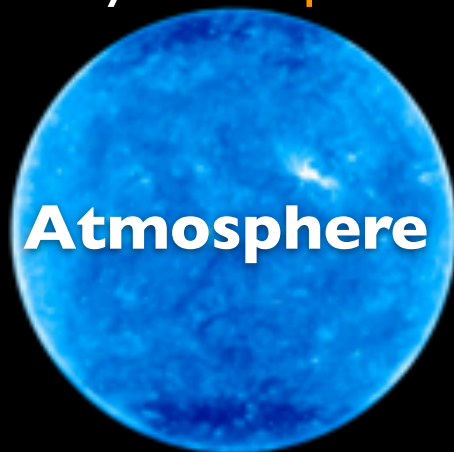


Mass loss and extension of the photosphere

Strong stellar wind causes the photosphere to be formed in the wind

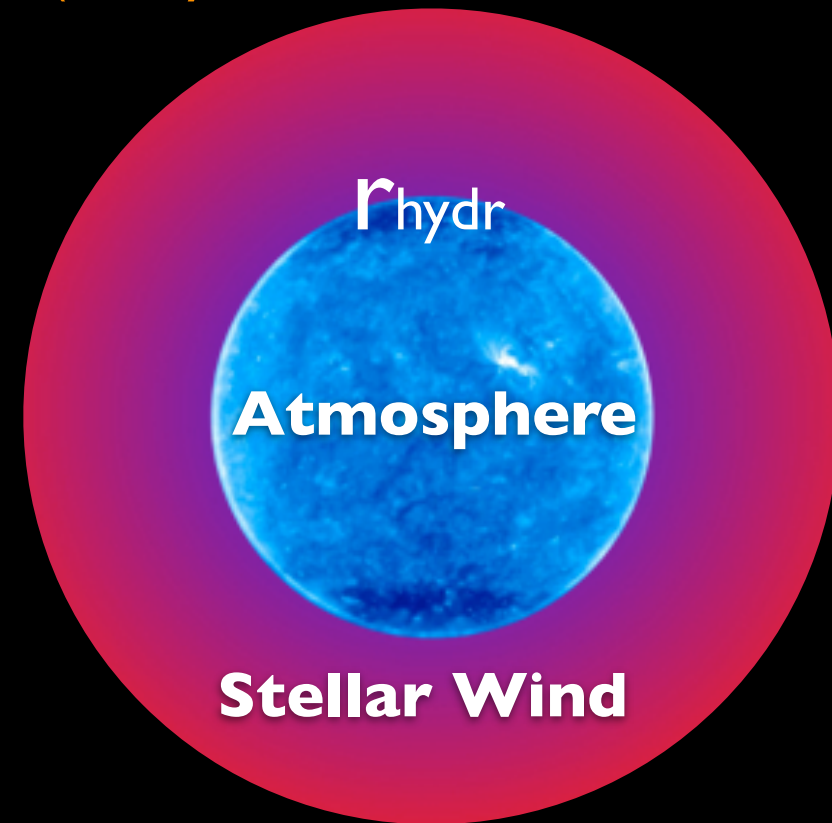
Sun

$$r_{\text{hydr}} = r_{\text{phot}}$$



Eta Car ($\dot{M}/2$)

r_{phot} (set by free-free emission in the K-band)

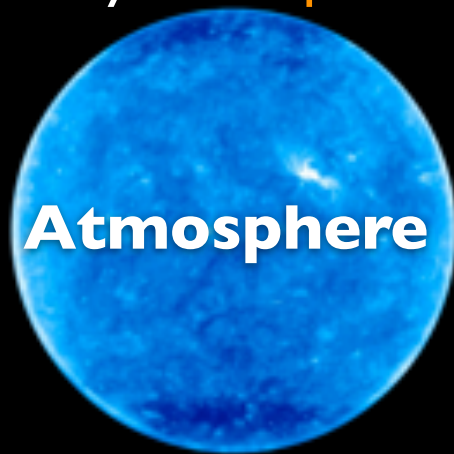


Mass loss and extension of the photosphere

Strong stellar wind causes the photosphere to be formed in the wind

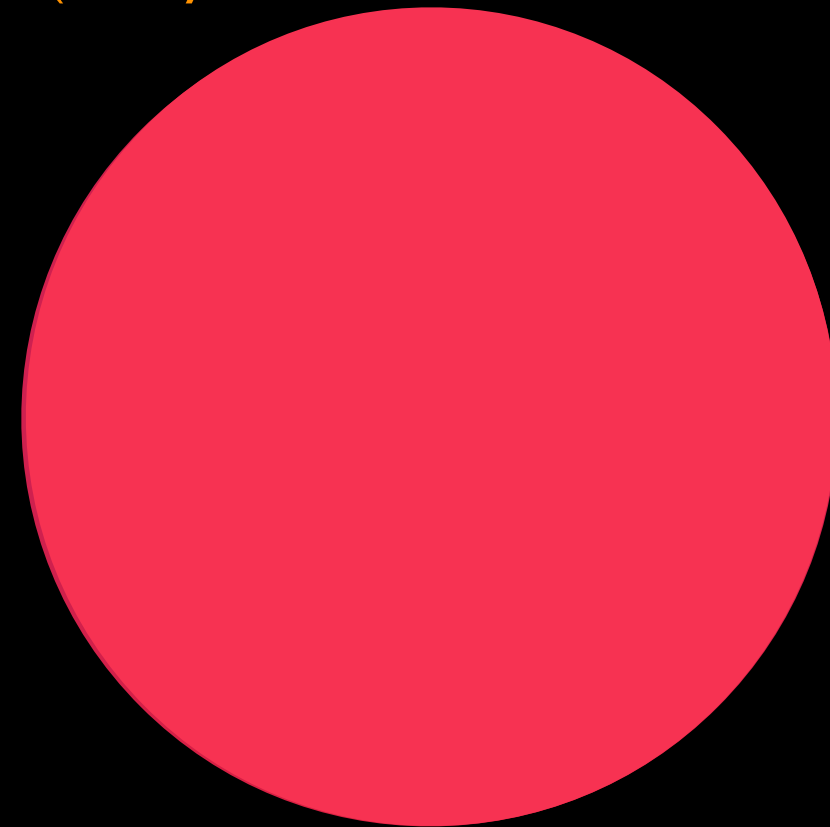
Sun

$$r_{\text{hydr}} = r_{\text{phot}}$$



Eta Car ($\dot{M}/2$)

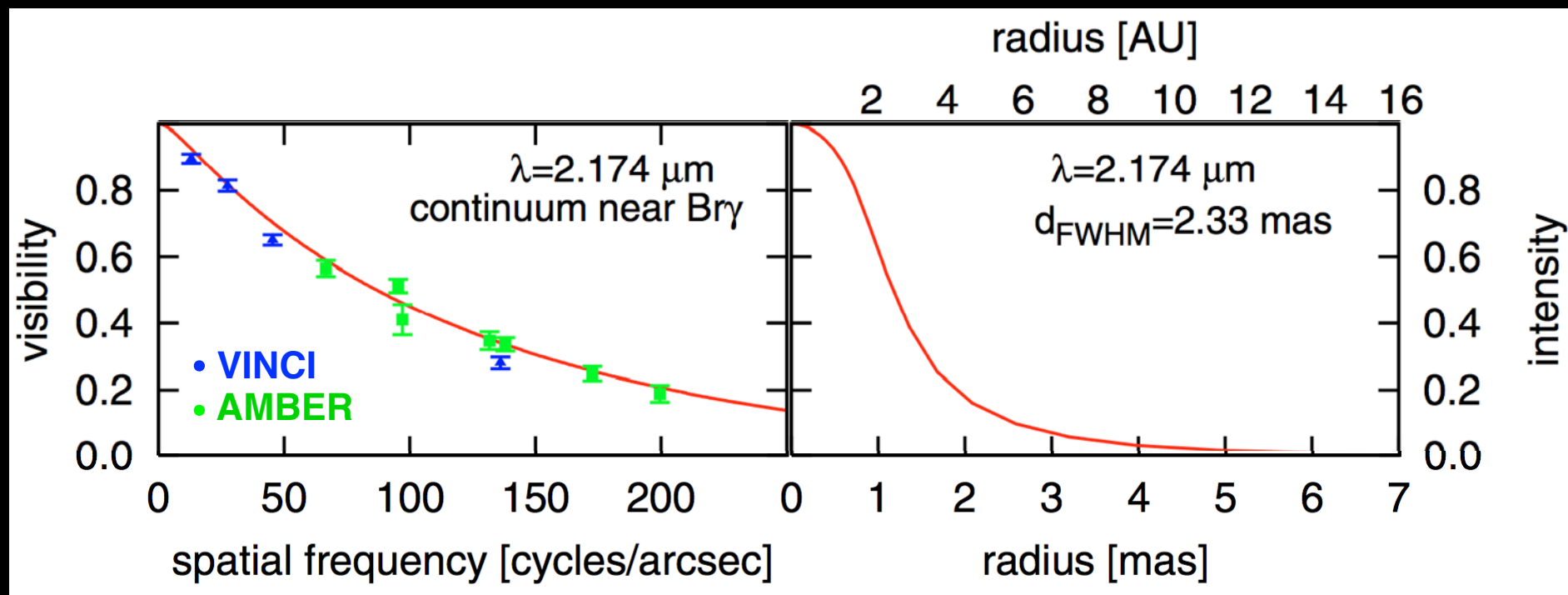
r_{phot} (set by free-free emission in the K-band)



Eta Carinae mass loss

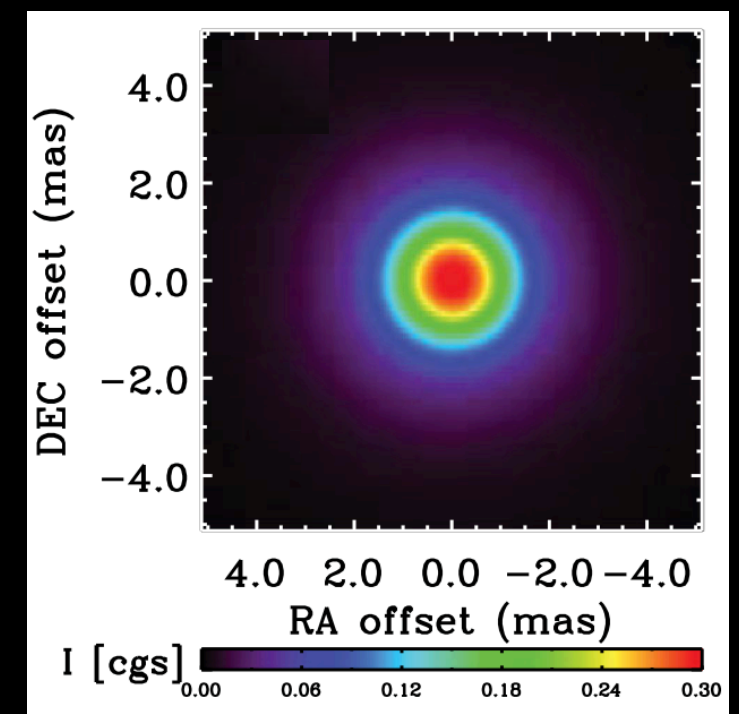
(van Boekel+03; Weigelt+07; Kervella 07; Groh+10, 12)

Observations



Weigelt+07

NLTE 1D model image

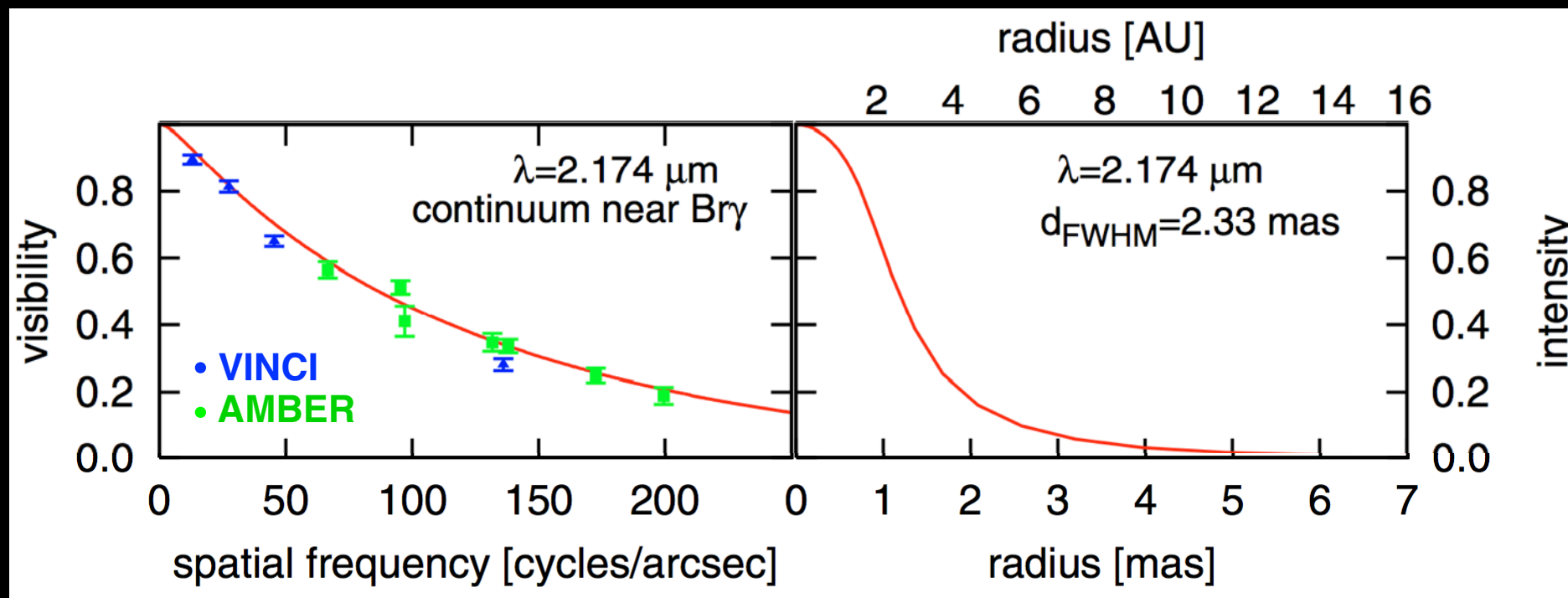


Groh+12

Eta Carinae mass loss

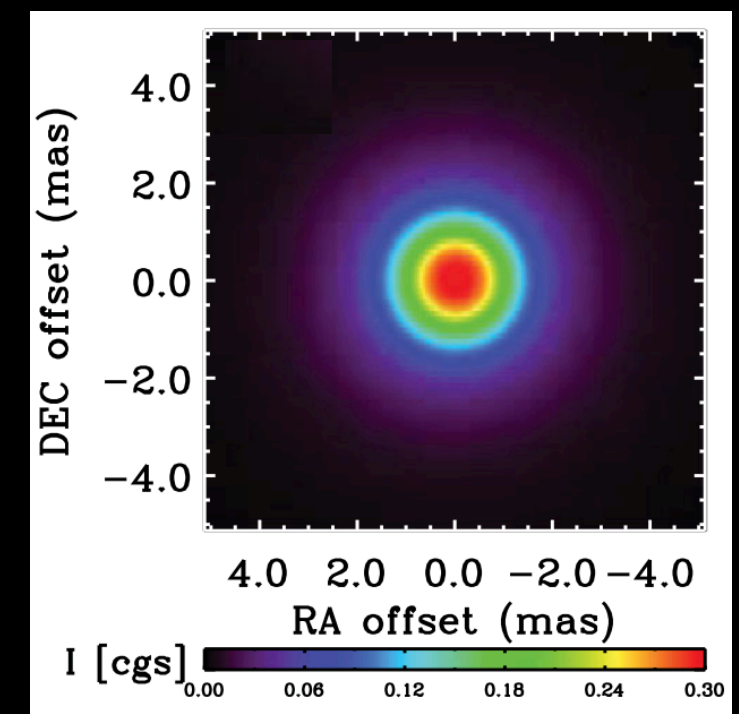
(van Boekel+03; Weigelt+07; Kervella 07; Groh+10, 12)

Observations



Weigelt+07

NLTE 1D model image



Groh+12

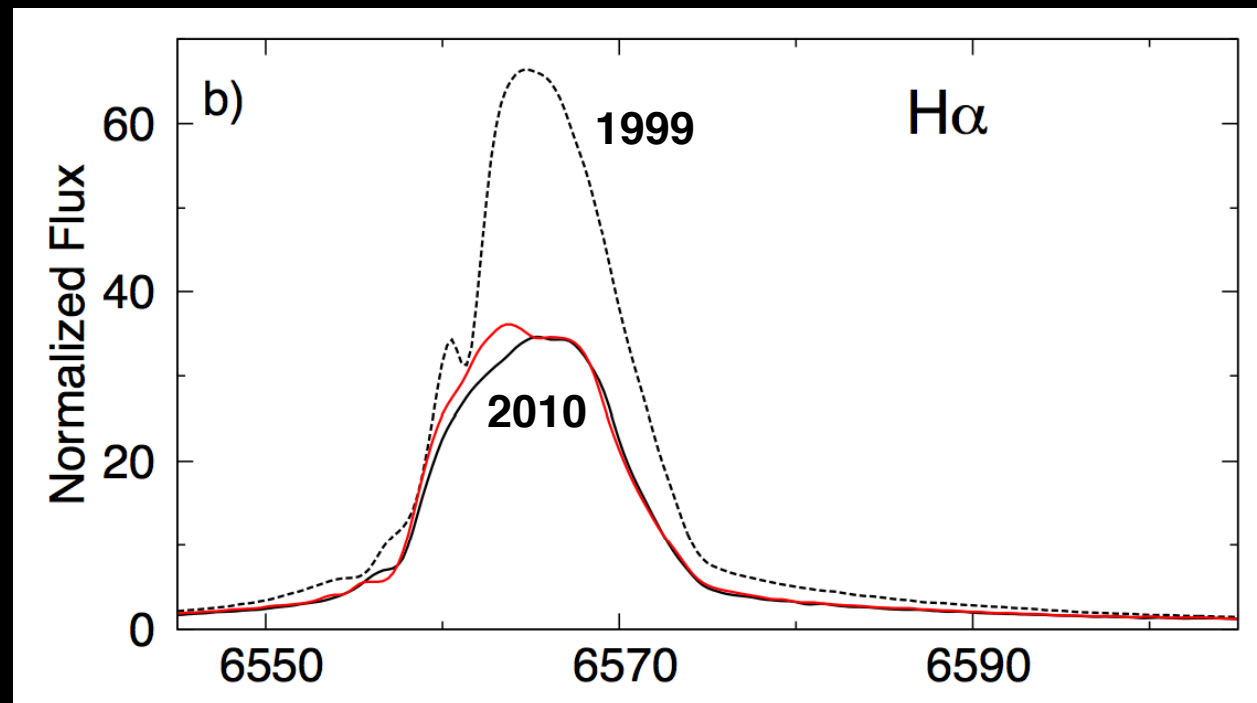
Mass-loss rate in 2002-2005: $\sim 8.4 \times 10^{-4} \text{ Msun/yr}$

Groh+12

Variability in Eta Carinae mass loss?

(Mehner+10, 12, 14 Corcoran+10, Gull+11, Groh+12a,b, Teodoro+12, Madura+13)

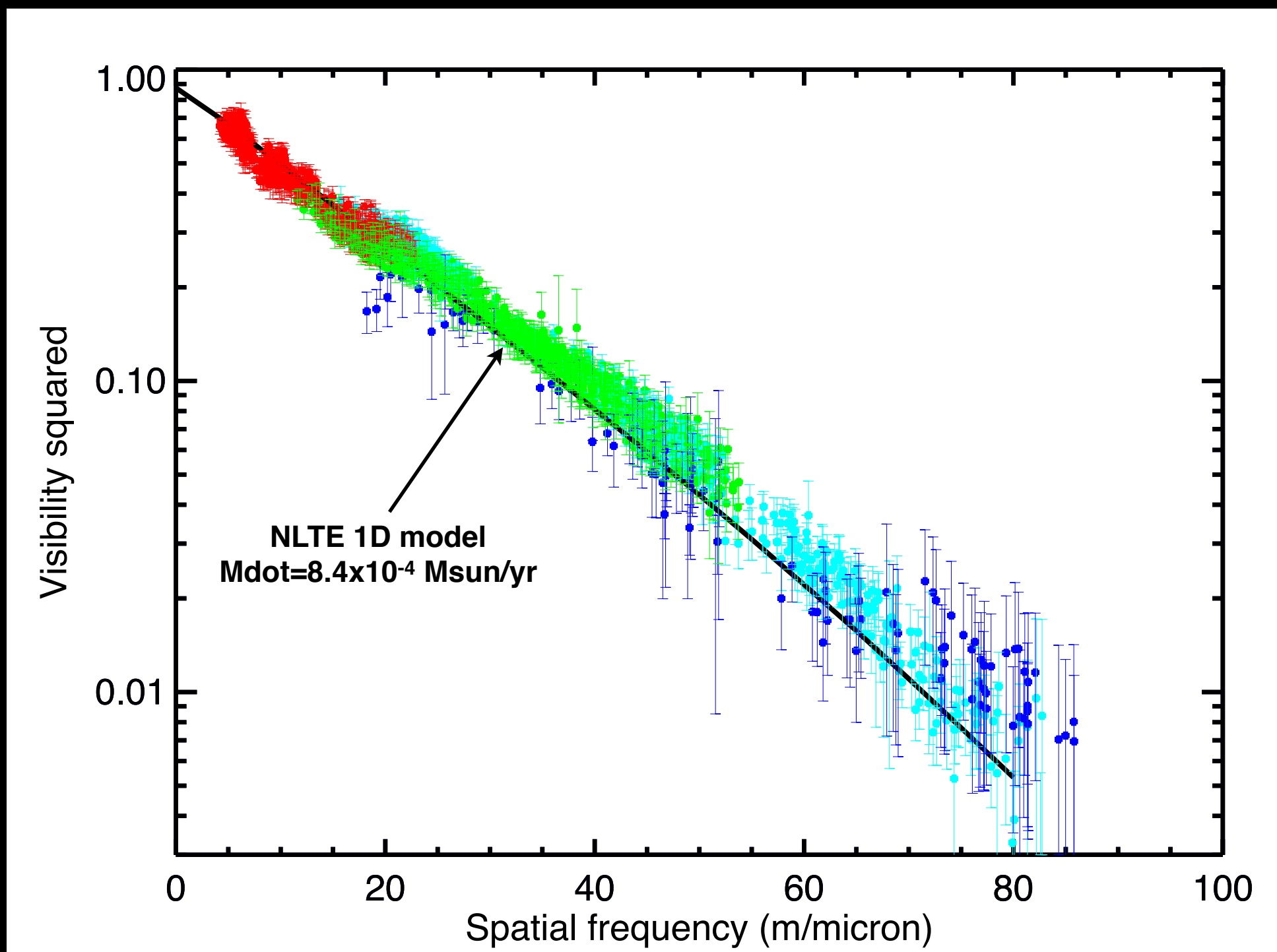
Mass-loss rate reduction by a factor of 2 in the last 10 yr?



Mehner+12

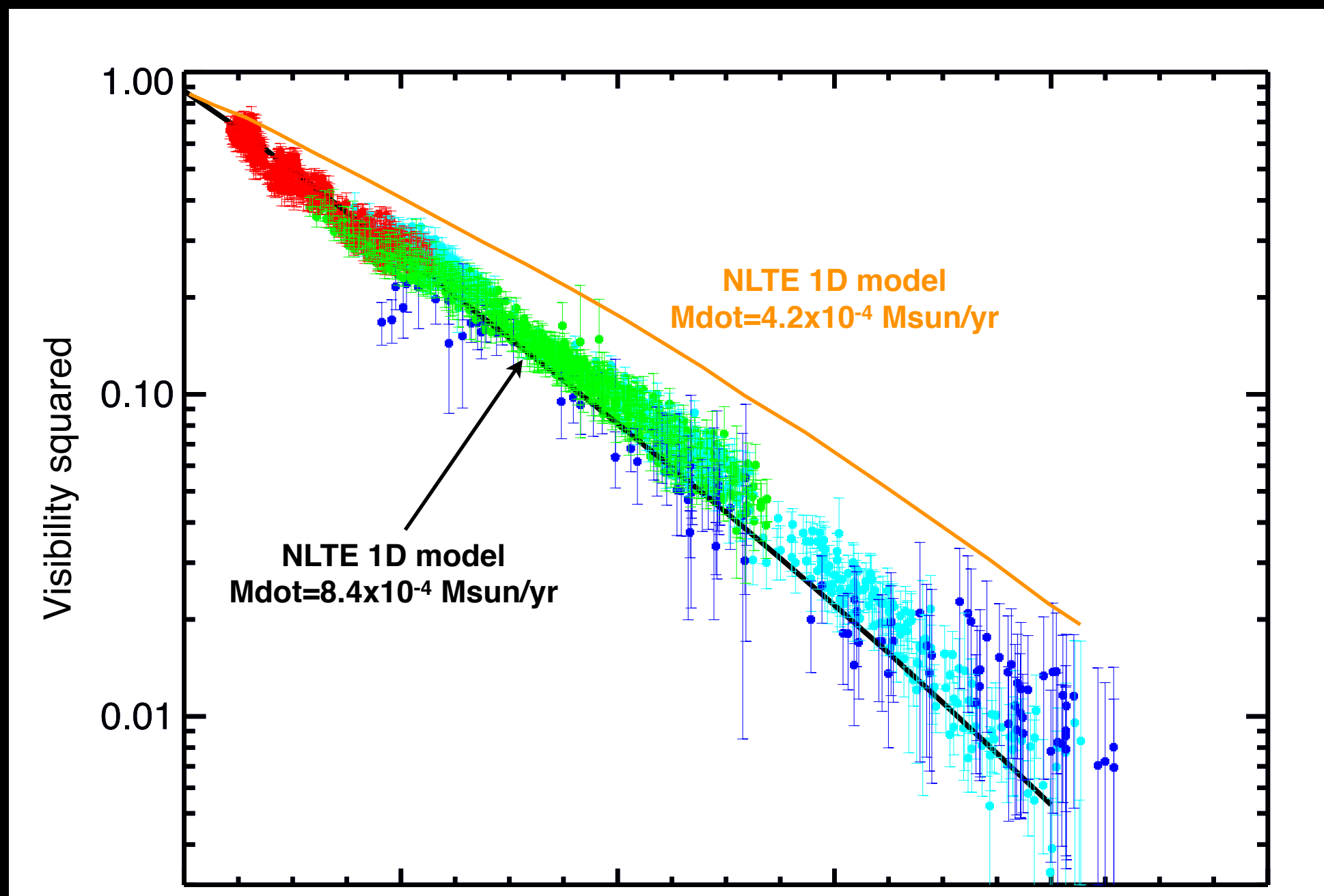
Probing changes in mass loss with VLT/PIONIER

Data taken by O. Absil on **2012 Mar** and **2013 Feb**



Probing changes in mass loss with VLTI/PIONIER

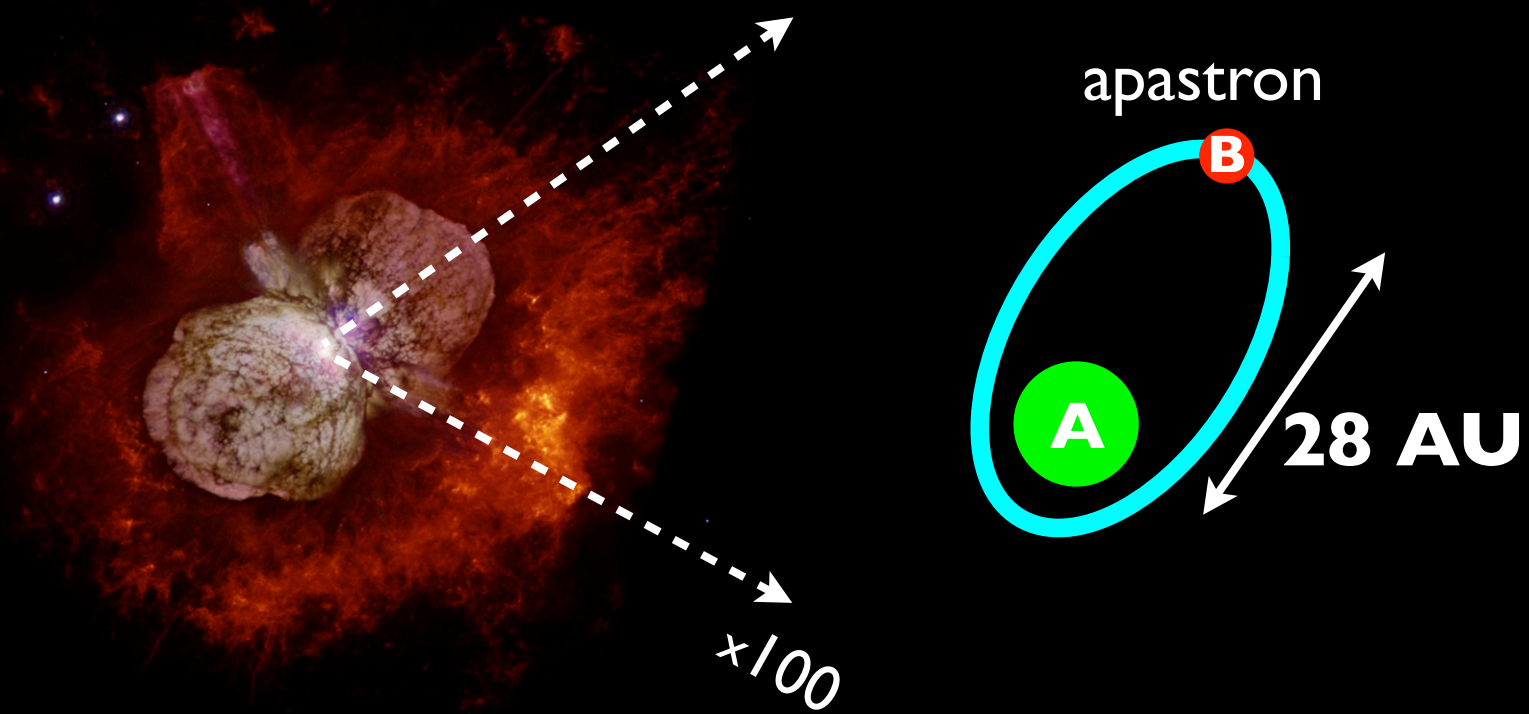
Data taken by O. Absil on **2012 Mar** and **2013 Feb**



PIONIER 2012-2013 data do NOT support a noticeable change in Eta Car's mass-loss rate.

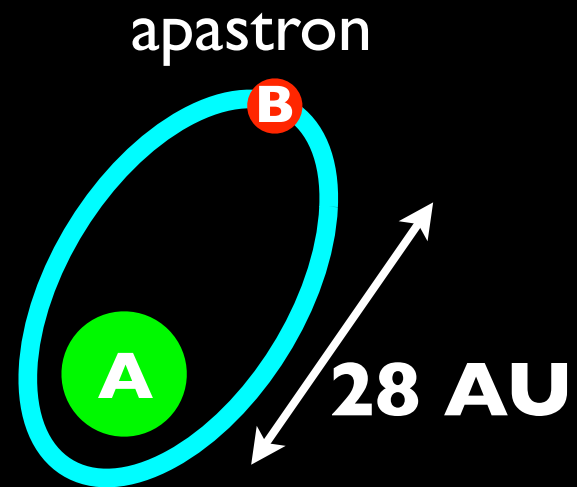
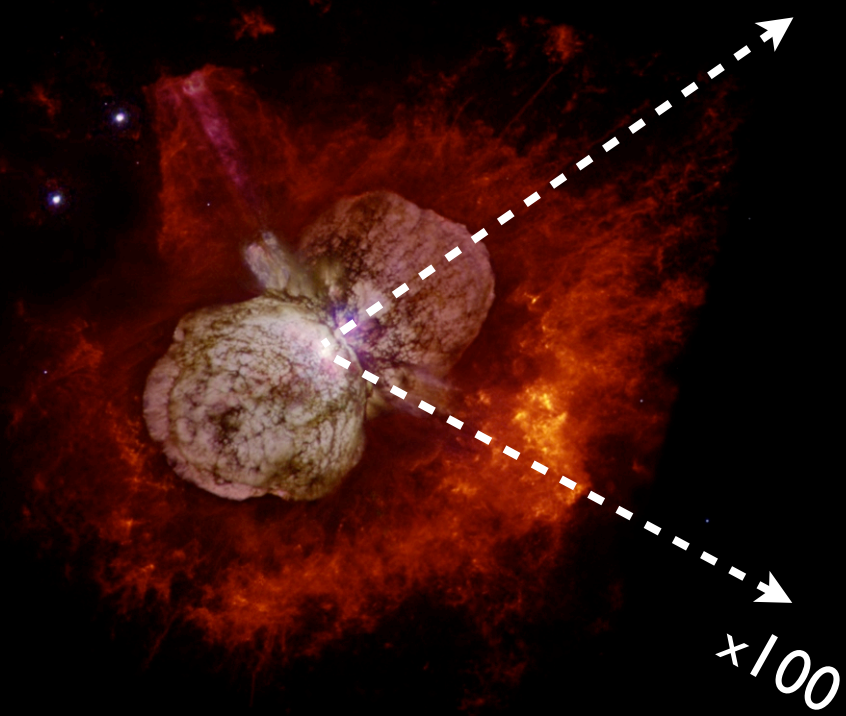
Binarity of Eta Carinae: effects are time dependent

Orbit: $i=139^\circ$, $\omega=243^\circ$, $PA=312^\circ$, $e=0.9$, $P=5.54$ years
(Damineli 96; Madura+ 12)

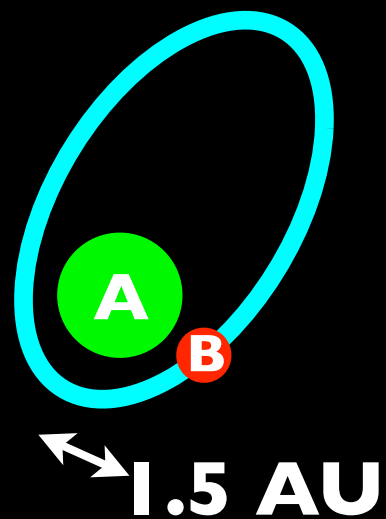


Binarity of Eta Carinae: effects are time dependent

Orbit: $i=139^\circ$, $\omega=243^\circ$, $PA=312^\circ$, $e=0.9$, $P=5.54$ years
(Damineli 96; Madura+ 12)



Around periastron



Effects of binarity in Eta Car

Changes in the density structure of the primary wind

Density cuts from 3D hydrodynamical SPH simulations of the Eta Car binary system (Madura + 13): orbital period $P=5.54$ yr, eccentricity $e=0.9$.



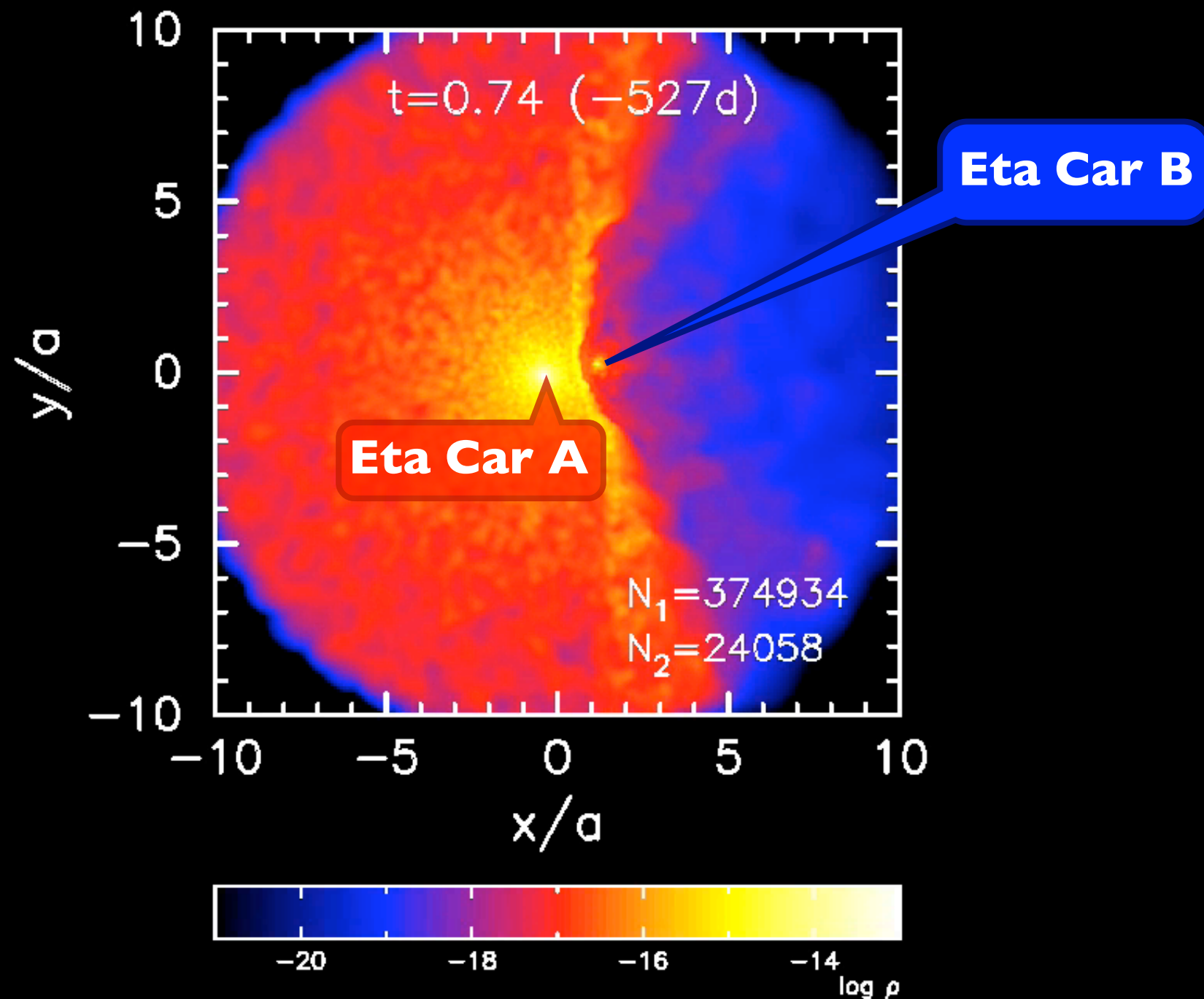
Eta Car A

Eta Car B

Effects of binarity in Eta Car

Changes in the density structure of the primary wind

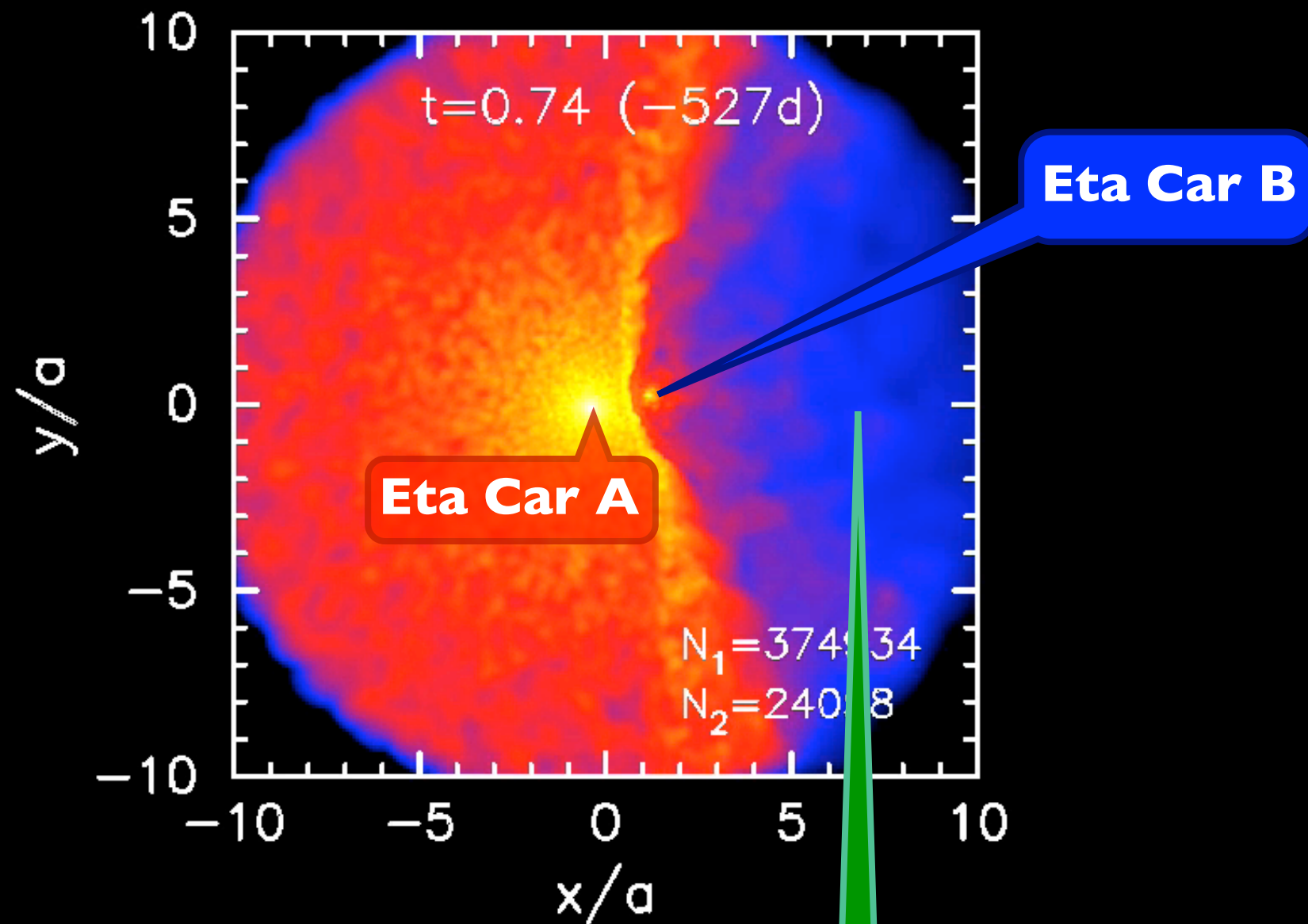
Density cuts from 3D hydrodynamical SPH simulations of the Eta Car binary system (Madura + 13): orbital period $P=5.54$ yr, eccentricity $e=0.9$.



Effects of binarity in Eta Car

Changes in the density structure of the primary wind

Density cuts from 3D hydrodynamical SPH simulations of the Eta Car binary system (Madura + 13): orbital period $P=5.54$ yr, eccentricity $e=0.9$.



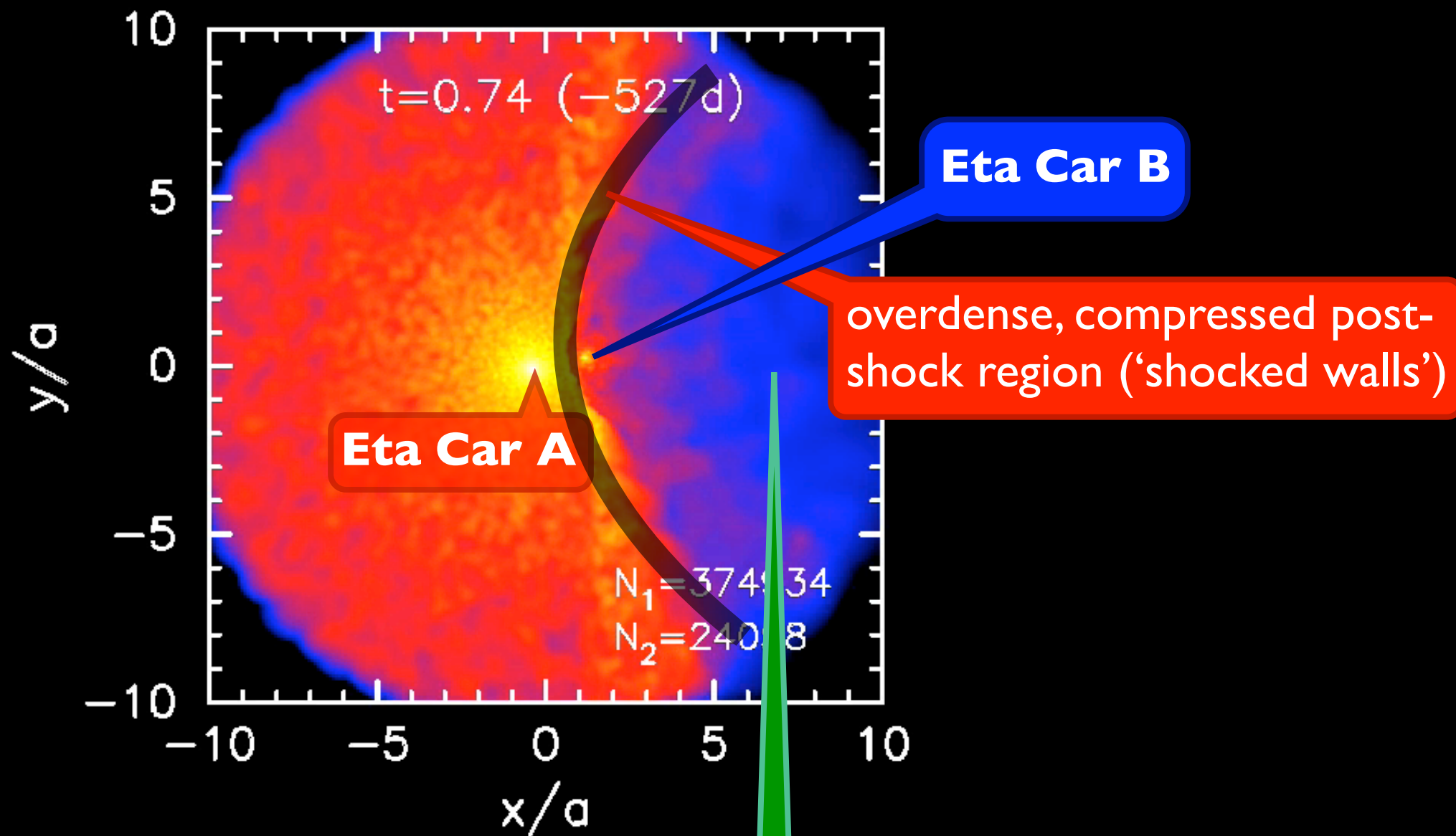
Fast wind of the companion produces a **cavity** in the dense wind of the primary star

(Pittard & Corcoran 2002, Okazaki+ 08, Parkin+ 09, 11; Madura+ 12, 13).

Effects of binarity in Eta Car

Changes in the density structure of the primary wind

Density cuts from 3D hydrodynamical SPH simulations of the Eta Car binary system (Madura + 13): orbital period $P=5.54$ yr, eccentricity $e=0.9$.



Fast wind of the companion produces a **cavity** in the dense wind of the primary star

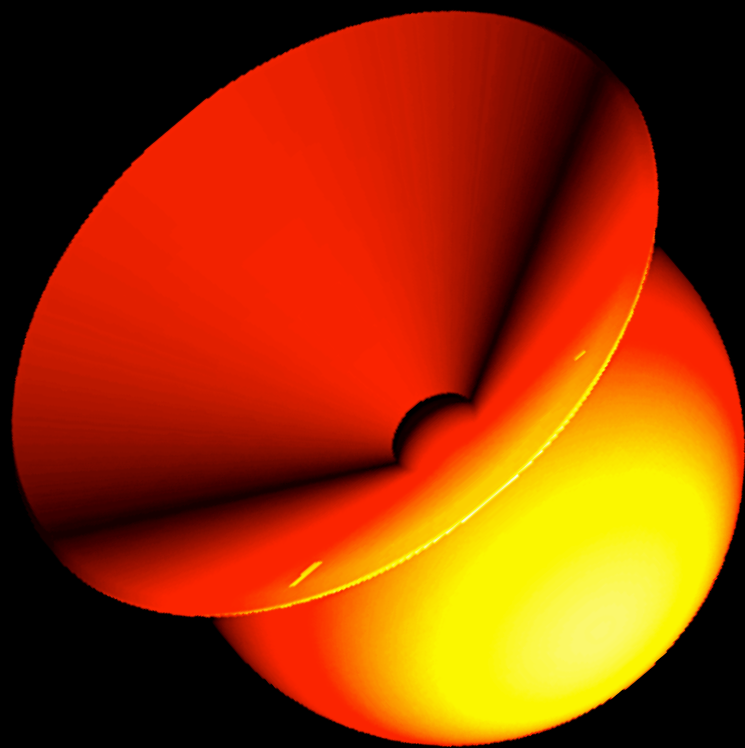
(Pittard & Corcoran 2002, Okazaki+ 08, Parkin+ 09, 11; Madura+ 12, 13).

Effects of the companion star on Eta Car

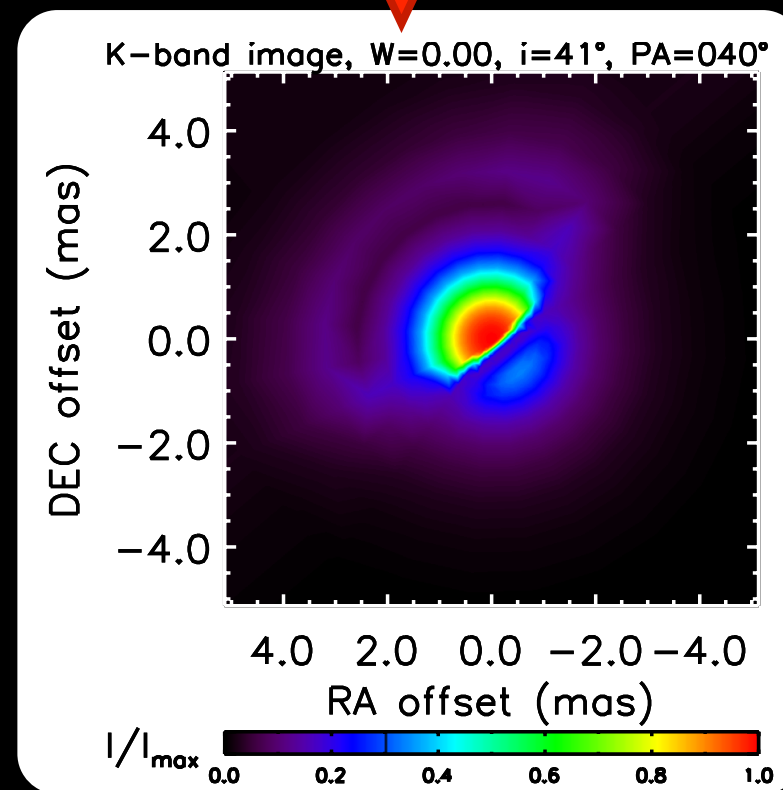
Near-infrared: geometry of the K-band continuum emitting region

A 2D model with $i=41^\circ$ (139°) and longitude of periastron of $\omega=243^\circ$ provides a reasonably good fit to the VINCI observations at orbital phase $\phi=0.93$.

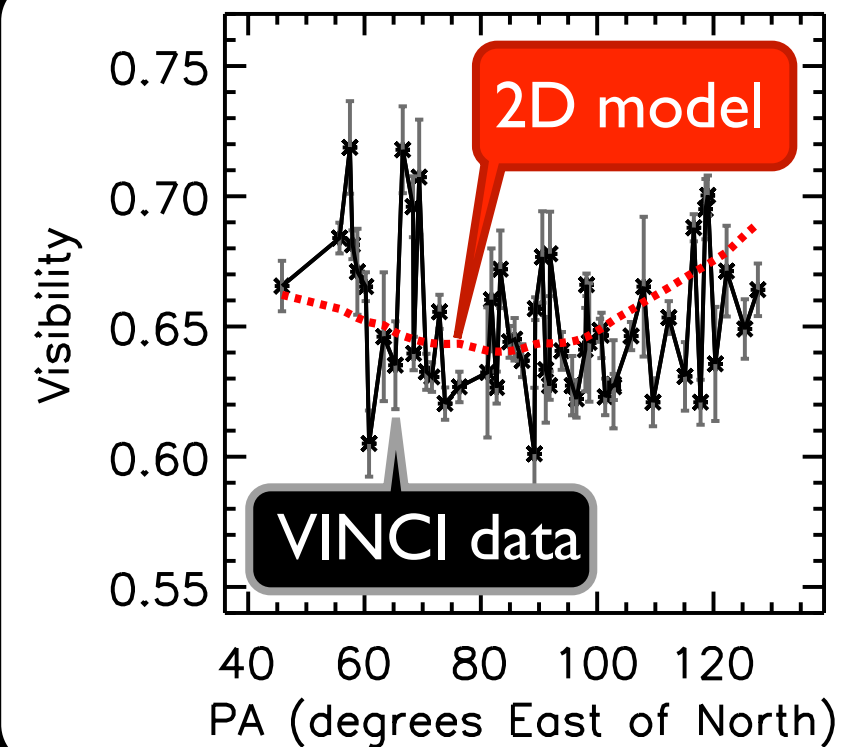
3-D isodensity surface



K-band continuum image



Fit to the visibilities



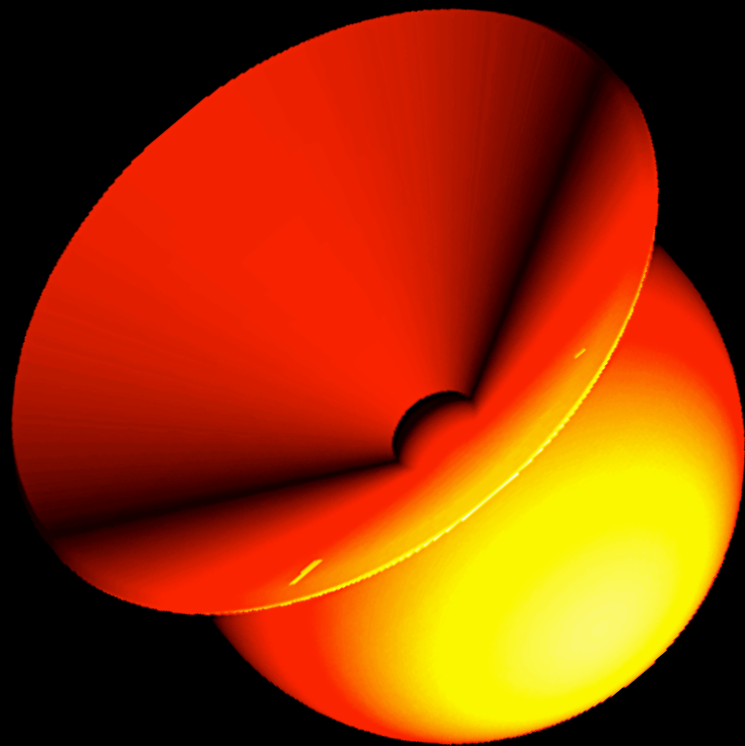
(Groh et al. 2010a)

Effects of the companion star on Eta Car

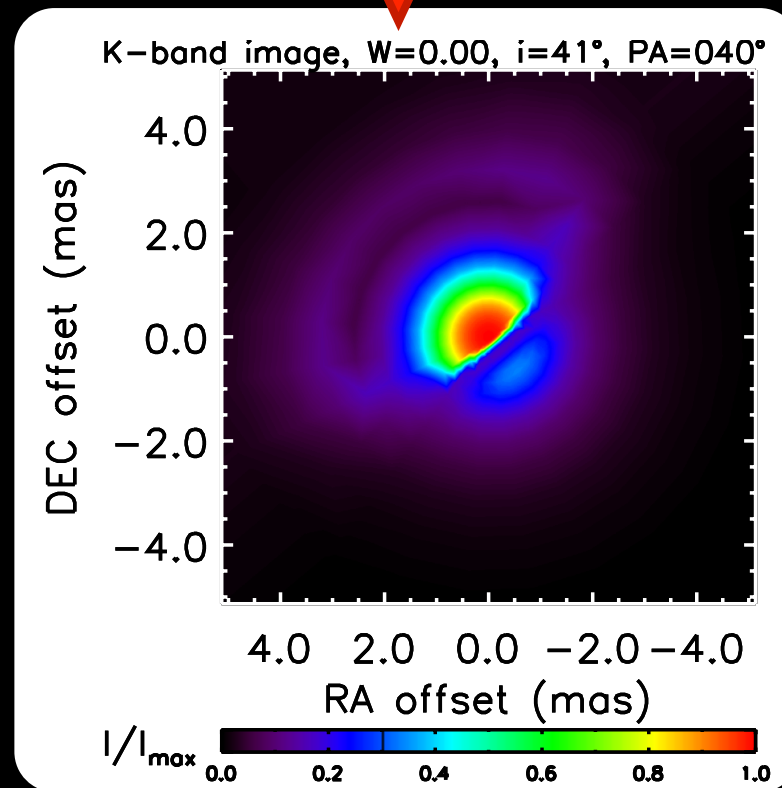
Near-infrared: geometry of the K-band continuum emitting region

A 2D model with $i=41^\circ$ (139°) and longitude of periastron of $\omega=243^\circ$ provides a reasonably good fit to the VINCI observations at orbital phase $\phi=0.93$.

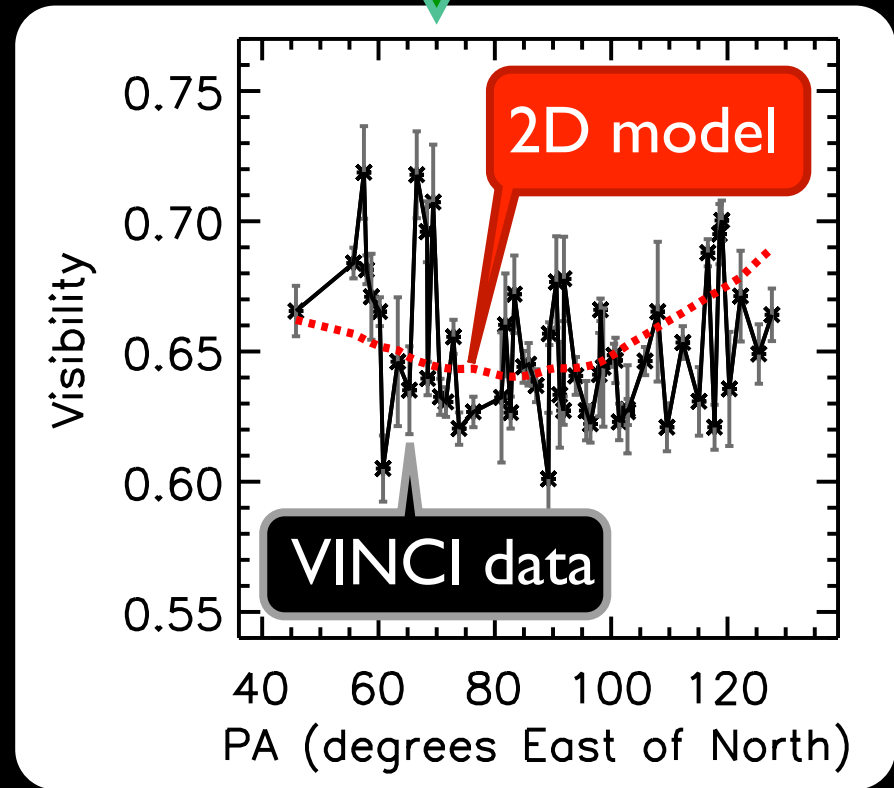
3-D isodensity surface



K-band continuum image



Fit to the visibilities



(Groh et al. 2010a)

Binary model fits data taken at periastron

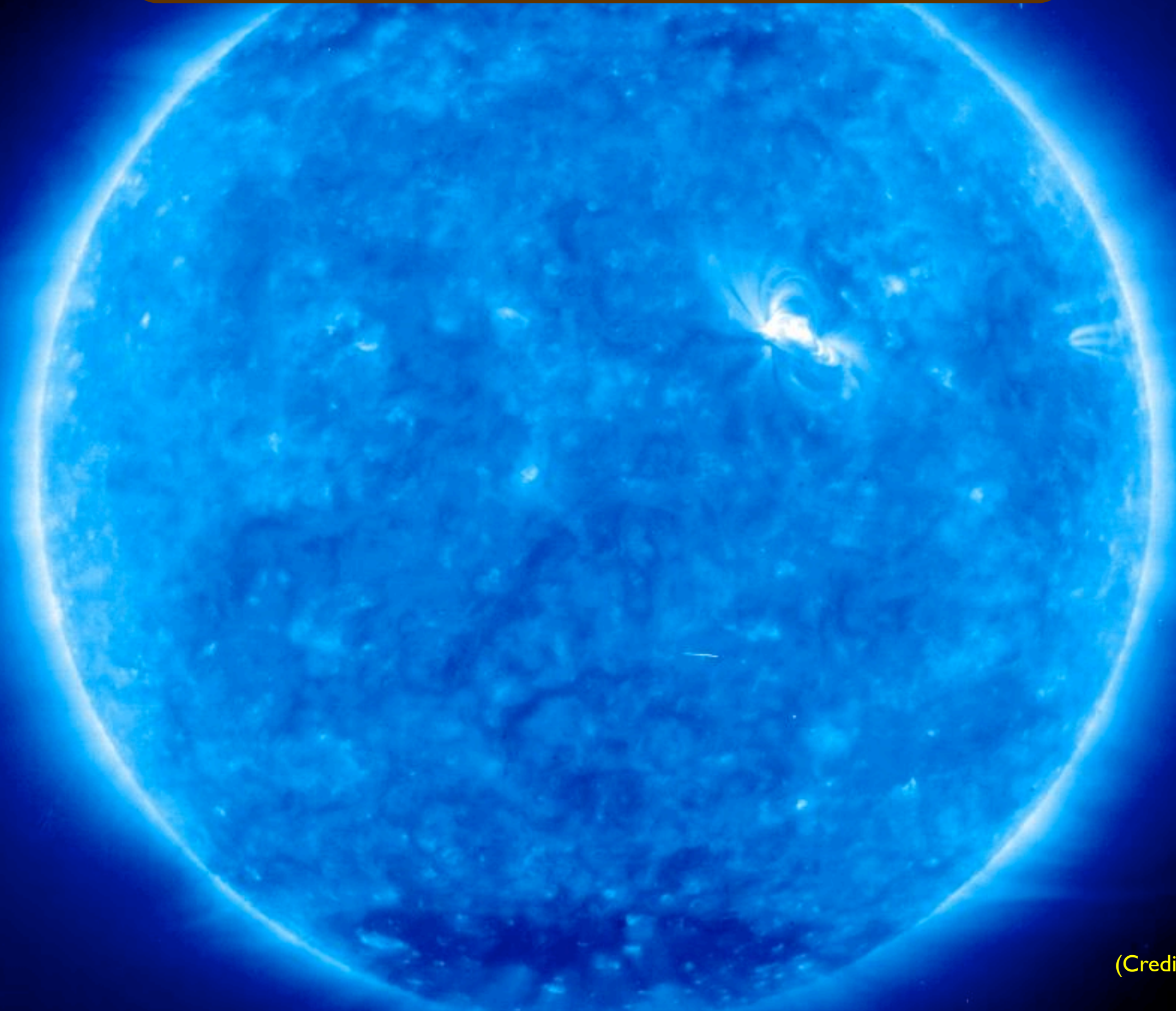
Take way messages

- **Interferometry is key to probe rotation, mass loss, and binary effects in massive stars**
- **Eta Carinae is key for understanding how O stars become WR stars and how LBVs explode as SNe**

Eta Carinae seen by interferometry:

- **no changes in \dot{M} over last 15 years;**
- **rapidly-rotating primary star (~80% critical speed) seem at $i \sim 60-90^\circ$ (misaligned with Homunculus);**
- **strong binary effects (WWC) around periastron.**

Interferometry is the way to go!



(Credit: NASA/ESA)